EXPLORING THE RELATIONSHIPS BETWEEN VEGETATION

MEASUREMENTS AND TEMPERATURE IN RESIDENTIAL AREAS BY

INTEGRATING LIDAR AND REMOTELY SENSED IMAGERY

A Thesis

by

MATTHEW A. CLEMONDS

Submitted to the Office of Graduate Studies of
Texas A&M University
in partial fulfillment of the requirements for the degree of

MASTER OF SCIENCE

August 2005

Major Subject: Geography

EXPLORING THE RELATIONSHIPS BETWEEN VEGETATION

MEASUREMENTS AND TEMPERATURE IN RESIDENTIAL AREAS BY

INTEGRATING LIDAR AND REMOTELY SENSED IMAGERY

A Thesis

by

MATTHEW A. CLEMONDS

Submitted to the Office of Graduate Studies of
Texas A&M University
in partial fulfillment of the requirements for the degree of

MASTER OF SCIENCE

Approved by:

Chair of Committee,	Hongxing Liu
Committee Members,	Robert Bednarz
	Daniel Sui
	John Nielsen-Gammon
Head of Department	Douglas Sherman

August 2005

Major Subject: Geography

ABSTRACT

Exploring the Relationships between Vegetation Measurements and Temperature in

Residential Areas by Integrating LIDAR and Remotely Sensed Imagery. (August 2005)

Matthew A. Clemonds, B.S., Texas A&M University

Chair of Advisory Committee: Dr. Hongxing Liu

Population growth and urban sprawl have contributed to the formation of significant urban heat island phenomena in Houston, Texas, the fourth largest city in the United States. The population growth in Houston was 25.8% between 1990 and 2000 nearly double the national average. The demand for information concerning the effects of urban and suburban development is growing. Houston is currently the only major US city lacking any kind of comprehensive city zoning ordinances.

The Normalized Difference Vegetation Index (NDVI) has been used as a surrogate variable to estimate land surface temperatures at higher spatial resolutions, given the fact that a high-resolution remotely sensed NDVI can be created almost effortlessly and remotely sensed thermal data at higher resolutions is much more difficult to obtain. This has allowed researchers to study urban heat island dynamics at a micro-scale. However, this study suggests that a vegetation index alone might not be the best surrogate variable for providing information regarding the independent effects and level of contribution that tree canopy, grass, and low-lying plants have on surface temperatures in residential neighborhoods. This research combines LIDAR (Light Detection and Ranging) feature height data and high-resolution infrared aerial photos to

measure the characteristics of the micro-structure of residential areas (residential-structure), derives various descriptive vegetation measurement statistics, and correlates the spatial distribution of surface temperature to the type and amount of vegetation cover in residential areas. Regression analysis is used to quantify the independent influence that different residential-structures have on surface temperature. In regard to implementing changes at a neighborhood level, the descriptive statistics derived for residential-structure at a micro-scale may provide useful information to decision-makers and may reveal a guide for future developers concerned with mitigating the negative effects of urban heat island phenomena.

DEDICATON

I want to dedicate this thesis to my wife and daughters. Without the love, understanding, guidance, and support of my wife, Ronda Jo, my college education would not have been realized, much less this research. She has not only been a loving wife; she has provided her intellectual spirit toward my studies, which has proven to be invaluable. Without this input, my work and accomplishments would be weak. Ronda has stood by me through all of the long days and nights that turned into long months and years. I consider it a privilege to be able to repay the steadfast support she has shown me over the past six years. Her faith, her love, and the pride she shows for me and my work has continuously motivated me and has provided me strength. I quite often worked imagining her looking over me, which pushed me to do the best work that I could without compromising. My daughters, Seabree Dyann and Kayla Shell, have been incredibly understanding. Evening after evening and weekend and weekend they have worked hard to allow me this time of learning. Their own educational accomplishments are a testament of their maturity and fortitude. They have patiently supported my education, and I look forward to spending much more time with both of them. My family has been an inspiration and a foundation. Thank you, from the bottom of my heart to Kayla, Seabree, and Ronda.

ACKNOWLEDGMENTS

Dr. Douglas Sherman, the head of the department of Geography, is a strong educator and researcher that has set a fantastic example and has motivated my work. Besides Dr. Liu, Dr Andrew Klein has taught me more about my area of study than any other professor. He has also worked hard at reviewing this research providing valuable insight. Dr. Sarah Bednarz has been amazingly supportive and has shown great confidence in my abilities. Dr. Jonathan Smith has shown me how to think bigger. The faculty and staff of Texas A&M University have been terrific; thank you.

I would also like acknowledge some of my colleagues. I want to personal thank Lei Wang for the many hours that he spent working with me. Without his technical expertise, this research would not have been successful. Jaehyung Yu has also provided a valuable source of experienced knowledge. The friendships of all of my fellow students have helped make my educational experience enjoyable and rewarding.

Finally, I want to thank my wonderful parents, Curtis and Lucy, for their support and loving guidance. They have been brilliant examples of hard work and thoughtful accomplishment. They believe in doing your best even when it is not required. Following that example has opened doors and has provided its own personal rewards.

TABLE OF CONTENTS

LIST OF FIGURES

LIST OF TABLES

CHAPTER I

INTRODUCTION

1.1. The urban heat island

Urban heating is one of the most well known forms of anthropogenic climate modification (Streutker, 2003). Built-up urban areas coupled with deforestation concentrate the heating effect. Urban heat islands are urban areas with air and surface temperatures higher than the ambient temperatures that are associated with their surrounding rural areas (Streutker, 2003; Montávez et al., 2000; Aniello et al., 1995). By calculating the temperature difference between the urban area and the surrounding rural area, the intensity of an urban heat island can be identified (Montávez et al., 2000). It has been shown that the urban heat island effect can be as high as 4 to 6.5° C (Streutker, 2002; Matson et al., 1978).

The urban heat island effect was first documented by Luke Howard during his studies regarding the climate of London over 170 years ago (Streutker, 2003; Howard, 1833; BMS, 2004). This effect became well recognized since the 1960s, when research revealed an increase in the annual high temperatures for the City of Los Angeles. Trees, citrus groves, and natural vegetative cover were replaced with buildings, parking lots, roads, and industrial and commercial complexes; the average temperatures in the downtown area of Los Angeles have increased by approximately 1° F each decade from the 1930s to the present (LBNL, 2004; Aniello et al., 1995).

_____

This thesis follows the style of *Remote Sensing of Environment*.

Many factors contribute to the formation of urban heat islands: the increasing area of dark surfaces that absorb relatively more heat (radiant energy) from the sun (Lo & Quattrochi, 2003); a concentration of per capita energy consumption in densely populated areas (Streutker, 2002), sometimes referred to as "anthropogenic heat flux" (Sailor et al., 2003); and a convective stagnation over larger cities that can exacerbate the problems associated with urban heat islands is yet another contributor (Mann, 1993). Although it is often difficult to develop a comprehensive list of contributors to the urban heat island effect, the removal of vegetation or deforestation and replacing it with concrete impervious surfaces is a well known factor (Jensen, 2000; Lo et al., 1997). Vegetative cover or tree canopy provides buildings with shade, intercepts solar radiation, and cools the air by evapotranspiration (Akbari, 2002; Lo & Faber, 1997; Aniello et al., 1995; Henry et al., 1989). Urban deforestation is strongly correlated with increasing population densities and the resulting urban sprawl (Lo & Faber, 1997). It is certainly true that humans play a major role in the transformation of the Earth's surface, "particularly through deforestation and urbanization" (Walsh et al., 2004: 492; Goudie, 2000).

Urban heating can have a negative impact on the economy and human health (Lo & Quattrochi, 2003). The higher temperatures of urban heat islands prompt an increase in the amount of energy used for air conditioning. Air conditioners themselves contribute significant amounts of heat energy into the urban environment (Jensen, 2000). Pollution levels and energy costs increase as power plants burn more fossil fuel in response to the higher temperatures (Akbari, 2002). Accordingly, areas suffering from urban heat island

effects are not only uncomfortably hot; they generally possess relatively lower air quality (Lo & Quattrochi, 2003). Researchers have also linked higher temperatures from urban heat islands to acute respiratory problems and the aggravation of asthma (Lo & Quattrochi, 2003; Cardelino & Chameides, 1990; EPA, 2002).

1.2. Urban heat island research and thermal remote sensing

Many climatological studies regarding urban heat islands have been performed using *in situ* data from weather station networks and automobile transects (Voogt & Oke, 1997; Montávez et al., 2000). Although *in situ* data have the advantage of high temporal resolution and a long historical record, the individual point measurements are commonly widely spaced and provide poor spatial coverage; and errors are introduced in the interpolation process, which is conducted to create a continuous surface dataset. More recently, remote sensing techniques have increasingly been employed in the study of urban heat islands, along with Geographic Information Systems (GIS). Remotely sensed data have higher spatial resolutions and can provide larger ground coverage than the individual point measurements from *in situ* data (Jensen, 2000).

Many satellite based urban heat island studies have been based on two thermal channels of AVHRR (Advanced Very High Resolution Radiometer) imagery (Price, 1984; Prata, 1993; Roth et al., 1989; Streutker, 2003; 2002). Landsat TM (Thematic Mapper) and ETM+ (Enhanced Thematic Mapper Plus) (Weng et al., 2004; Kawashima et al., 2000) and airborne ATLAS (Advanced Thermal and Land Applications Sensor) thermal imagery have been used to derive land surface temperatures at a greater spatial

resolution than that provided by the AVHRR. The Global Hydrology and Climate Center of the National Aeronautic and Space Administration (NASA) has used the ATLAS to acquire thermal imagery at a much higher spatial resolution (up to 5 meters); however, this data has only been obtained for a small number of cities in the United States: Atlanta, Baton Rouge, Sacramento, and Salt Lake City (Stone & Rodgers, 2001; Quattrochi et al., 2000; Lo et al., 1997; GHCC, 1997; ATLANTA, 2004). At this resolution, the thermal emission of a single parcel can be measured (Stone & Rodgers, 2001; Lo et al., 1997).

Researchers have utilized thermal remote sensing data to analyze the correlations between surface temperature and various surface characteristics. Lo et al. (1997), Gallo & Tarpley (1996), and Roth et al. (1989) used remote sensing techniques to compare the urban heat island effect to vegetation coverage, which is often measured by the Normalized Difference Vegetation Index (NDVI). Owen et al. (1998) used fractional vegetation cover and surface moisture availability to study the impact of urban growth on surface radiant temperature of a region near State College, PA over a 10 year period. Yamshita & Sekine (1990), Nichol (1996), Sakakibara (1996), and Oke (1987) examined the influence of urban geometry and morphology on the urban heat island effect.

Remote sensing technology is broadening research by providing researchers with the ability to examine large areas of terrain in greater and greater detail (Jensen, 2000). It is possible to obtain a vegetation index with an extremely fine spatial resolution from aerial photography or obtain Digital Elevation Models (DEMs) from airborne LIDAR (Light Detection and Ranging) data with about 5 meter spatial resolution. However, the

thermal infrared sensors that are most commonly used to derive surface temperatures have relatively poor spatial resolutions (Table 1.1) compared to the visible and near-infrared bands of some of the most common sensor platforms (Kustas et al., 2003; Campbell, 2002). Therefore, the study of urban heat islands at a micro-scale with thermal remote sensing has often been limited. Methods used to achieve more detailed spatial resolutions in regards to temperature and urban heating studies frequently employ the strong negative correlation between vegetation and surface temperature (Lo et al., 1997). Because the availability of high-resolution thermal data is so scarce, many researchers have examined the use of vegetation measurements (e.g., NDVI), remotely sensed at a more detailed spatial resolution, as a surrogate for thermal data, which are remotely sensed at a more coarse spatial resolution (Li et al., 2004; Weng et al., 2004; Kustas et al., 2003; Lo & Faber, 1997; Gallo & Tarpley, 1996; Roth et al., 1989).

Table 1.1
Common Thermal Sensors

Sensor	Spatial Resolution (m)
GOES	4000
AVHRR	1100
MODIS	1000
Landsat 5 TM	120
ASTER	90
Landsat 7 ETM+	60

The spatial resolution of airborne LIDAR data is exceptionally fine: the average density of the laser pulses can be as high as 1 meter on the ground; and the vertical accuracy is as high as about 15 cm, due to the fact that the aircraft uses a differential Global Positioning System (GPS) and an Inertial Measuring Unit (IMU) to obtain the

precise position and attitude of the onboard laser sensor (Campbell, 2002; Jensen, 2000; Flood & Gutelius, 1997; Krabill et al., 1984). From these LIDAR data, detailed DEMs can be created (Maas, 2002; Krabill et al., 1984). However, the majority of the LIDAR measurements (laser pulses) do not reach the ground in areas with significant tree canopy or man-made structures (Jensen, 2000). Although this may sometimes present a problem, it can also be an advantage to receive measurements from both the ground and the vegetation or man-made structures simultaneously. With a considerable amount of processing of the raw LIDAR data, "bald-Earth" DEMs *and* vegetation heights can be derived (Clark et al., 2004; Persson et al., 2002; Krabill et al., 1984). The use of Digital Canopy Models (DCMs) obtained from LIDAR technology has made it possible to estimate biomass, tree heights, stand volume (Nilsson, 1996; Nelson et al., 1988), and even delineate individual tree crowns (Clark et al., 2004; Brandtberg et al., 2003; Persson et al., 2002). Although very few, if any, studies regarding urban heat islands have used LIDAR data, the high level of spatial detail that it provides has proven useful in this research of urban heat islands at a micro-scale.

One of the few urban heat island studies completed in Houston, Texas was carried out by Streutker (2003; 2002), who utilized a time series of AVHRR images to depict the development of the urban heat island of the city by quantifying its spatial extent and magnitude. However, due to the coarse spatial resolution (1.1 kilometers) of AVHRR data, the surface temperature patterns derived by Streutker lack spatial detail. He recommends continued monitoring of the Houston urban heat island and further research with greater geographical detail. While his research effectively focused on the

urban heat island for the Houston Metropolitan Area as a whole, he acknowledges the need to conduct research at greater spatial resolutions, "such as that of individual neighborhoods," to better quantify the causes of urban heat island phenomena (Streutker, 2003: 288). This thesis is focused in this apparent gap in urban heat island studies.

1.3. Research scope and objectives

This research explores urban heat islands at a micro-scale and the structure of residential areas in the Houston Metropolitan area by utilizing the relatively higher spatial resolution provided by aerial photography and LIDAR data, together with satellite imagery from Landsat ETM+ (Enhanced Thematic Mapper Plus). Using remote sensing techniques, GIS, and statistical methods, the objectives of this study include:

1) Combining and expanding upon research regarding the analysis and mapping of urban heat islands at a micro-scale and the mitigating effects of vegetation cover;

2) Developing micro-scale tree canopy and low-level vegetation (grass and low-lying plant) measurements to study urban heat island effects at the residential neighborhood level;

3) Measuring aspects of micro-structure of residential areas (residential-structure) using regression analysis and correlating these to surface temperature;

4) Evaluating the effectiveness of the micro-scale measurement approach as a better surrogate for explaining surface temperatures for residential neighborhoods; and

5) Examining the planning and policy implications regarding residential land development focused on residential-structure.

This research endeavors to identify the primary factors contributing to the formation of urban heat islands at a micro-level and examines what methods of development might be employed to mitigate (or at least not contribute to) the increased temperatures associated with the phenomena. By way of combining and expanding upon research regarding the analysis and mapping of micro-urban heat islands and the mitigating effects of vegetation cover (Lo & Quattrochi, 2003; Stone & Rodgers, 2001; Saaroni et al., 2000; Aniello et al., 1995), this research quantifies the relationships between vegetation cover, tree canopy, development, and temperature. Micro-urban heat islands or "hot spots" have been shown to radiate out from individual center points lacking tree canopy (Aniello et al., 1995). By utilizing feature heights derived from LIDAR data and a high-resolution NDVI derived from aerial photography, this research delineates and measures tree canopy and low-level vegetation cover independently for residential areas. This may provide a valuable tool to study urban heat island effects at a micro/neighborhood scale.

Large scale studies have eloquently defined and measured the urban heat islands for whole cities (Streutker, 2003; 2002; Lo & Quattrochi, 2003). Through micro-level analysis focused in residential areas, however, this research is aimed at providing a scientific basis for urban planning programs that can be implemented at the neighborhood level, related to the planned planting of trees and new land development styles to reduce urban and suburban heating. Employing remote sensing data, GIS, and correlation and regression statistical methods, this study analyzes and quantifies the relationships between micro-urban heat islands and vegetation specifically in regards to

the structure of residential areas. The utilization of LIDAR data and a high-resolution NDVI in this study elucidates the role of tree canopy, grass, and low-lying plants in reducing the land surface temperature increases associated with urban and suburban development. It has been suggested that high-resolution mapping of tree canopy may prove beneficial in defining and identifying the micro-urban heat island effect (Aniello et al., 1995). This research measures the micro-structure of residential areas (residential-structure), derives descriptive vegetation statistics, and correlates the spatial distribution of surface temperature and the type and amount of vegetation cover in residential areas.

Inasmuch as researchers have utilized vegetation indices as a surrogate for temperature, this research also utilizes the relationships between land-use and land-cover (LULC) classes, a 30-meter resolution NDVI image, and temperature to examine the larger spatial-scale urban heat island effect and its correlation to vegetation and LULC types. This larger spatial-scale analysis is compared to the residential-scale focus of this research, which concentrates on a micro-scale measurement approach using LIDAR data and a high-resolution NDVI image for neighborhoods. This comparison is then used to evaluate the effectiveness of the micro-scale vegetation measurement approach as a better surrogate than a vegetation index alone for providing information regarding the independent effects and level of contribution that tree canopy, grass, and low-lying plants have on surface temperatures in residential neighborhoods. The descriptive statistics derived to define the residential-structure at a micro-scale may provide useful information to decision-makers with respect towards planning and policy implementation regarding residential land development.

CHAPTER II

STUDY AREA: HOUSTON, TEXAS

2.1. Urban growth and heat island

Increases in urban population and the resulting urban sprawl have contributed to the formation of significant urban heat islands for nearly all of the larger cities of the world. In addition, most large cities are only growing larger. Houston is the 4th largest city in the United States in terms of population. The population growth of the Houston PMSA (Primary Metropolitan Statistical Area) was 25.8% between 1990 and 2000, which is nearly double that of the national growth rate of 13% (U.S. Census Bureau, 2001; 2000; 1995). The Houston PMSA consists of Harris County (the county in which the city of Houston is located) and a number of surrounding counties: Chambers, Fort Bend, Liberty, Montgomery, and Waller (U.S. Census Bureau, 1999).

Valuable oil well strikes near the city and the excellent ocean access that it enjoys has welded Houston's economy to the oil industry and has made the city an oil capital. This has launched rapid growth in the Houston area, especially in the last half of the 20th century (Figure 2.1). Dense population and economic activity has also triggered a rapid expansion of the area's urban and suburban built-up regions. However, Houston is currently the only major city in the United States lacking any kind of comprehensive city zoning ordinances (Streutker, 2003). Therefore, market forces generally drive commercial location decisions and not purposeful planning that might optimize the urban environment and avoid structural and functional design failures (Gregory, 2000).

Urbanization and the accompanying deforestation that takes place to make room for development are two of the major human processes acting to change the patterns of land-use and land-cover (LULC), and these "massive urban agglomerations" greatly influence the biosphere and the regional urban environments in which an ever growing percentage of the world's population resides (Berry, 1990: 117). The historical transformation of the Houston Area landscape from sparsely inhabited prairie, forest, and estuarine marsh to a sprawling moderately impervious urban surface created and increased the urban heat island effect (HARC, 2004; Streutker, 2003).
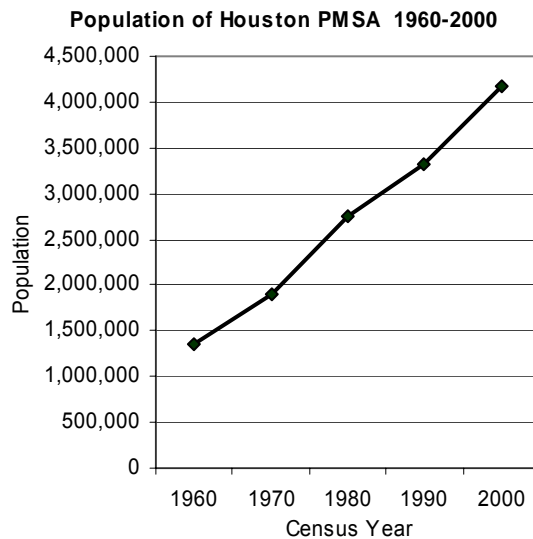
Figure 2.1. Population increases for the Houston PMSA from 1960 to 2000.

2.2. Heat and pollution

Research suggests that air quality and the quality of the environment are negatively affected by the urban heat island phenomenon (Lo & Quattrochi, 2003;

Cardelino & Chameides, 1990). Located in the sun-belt, Houston is characterized by relatively high temperatures and high humidity. The urban heat effect combined with the naturally warm environment of this southern city has increased the rate at which Volatile Organic Compounds (VOCs) and Nitrogen Oxides (NOx) combine in an aerial photochemical reaction to form ozone (EPA, 2002; Cardelino & Chameides, 1990). Houston has a recent unsavory history regarding adherence to the United States Environmental Protection Agency's (EPA) ozone and air particulate level standards. This low air quality is often visible in the form of smog, which is partly created by aerial photochemical reactions of pollutants like Volatile Organic Compounds (VOCs) and Nitrogen Oxides (NOx). Ground level ozone is produced from VOCs and NOx in the presence of sunlight (Lo & Quattrochi, 2003). These photochemical reactions are more frequent and intense at higher temperatures (Quattrochi et al., 2000; Cardelino & Chameides, 1990). Trees act not only to directly absorb polluting gases (NOx, sulfur oxides, particulate matter, and ozone) from the air; they also cool the environment, thus slowing the rate of the aerial photochemical reactions that create harmful ozone (Lo & Quattrochi, 2003).

One of the points of law and federal regulation that has come from the 1990 Clean Air Act and its amendments is the continued refinement of a spatial delineation referred to as a nonattainment area (CAA, 2004). It is defined as "any area that does not meet (or that contributes to ambient air quality in a nearby area that does not meet) the national … ambient air quality standard for [a] pollutant" (CAA, 2004). After passage of the Clean Air Act, national ambient air quality standards were set by the EPA for six air

pollutants: ozone, lead, carbon monoxide, sulfur dioxide, nitrogen dioxide, and respirable particulate matter (TNRCC, 2004a). The multi-county nonattainment area is somewhat akin to the multi-county PMSA. The federal laws that govern environmental compliance within nonattainment areas are more stringent. Accordingly, businesses in a nonattainment area are "subjected to stricter pollution control regulations" (Tannenwald, 1997: 87). These standards are applied across the board, and many smaller businesses and institutions that contribute very little to the pollution problem must also invest in adhering to complex compliance issues. Adhering to the more rigorous regulations increases the cost of conducting business and can be an economic burden to not only the business but the potential employee as well (Tannenwald, 1997).

There are sixteen ozone nonattainment counties in Texas, and eight of the counties are in the Houston/Galveston area. From 1997 to 1999 the 8-hour ozone standards were not met at any of the ozone monitoring stations in the Houston Metropolitan Area, which is in the Houston/Galveston Nonattainment Area, illustrated by Figure 2.2 (EPA, 2000; TNRCC, 2004b). This research concentrates on a select number of residential neighborhoods within Harris County, but the policy implications regarding the impact that residential-structure has on regional temperatures for this study could provide information that ultimately relieves economic burdens by reducing overall temperatures, energy consumption, and pollution levels.
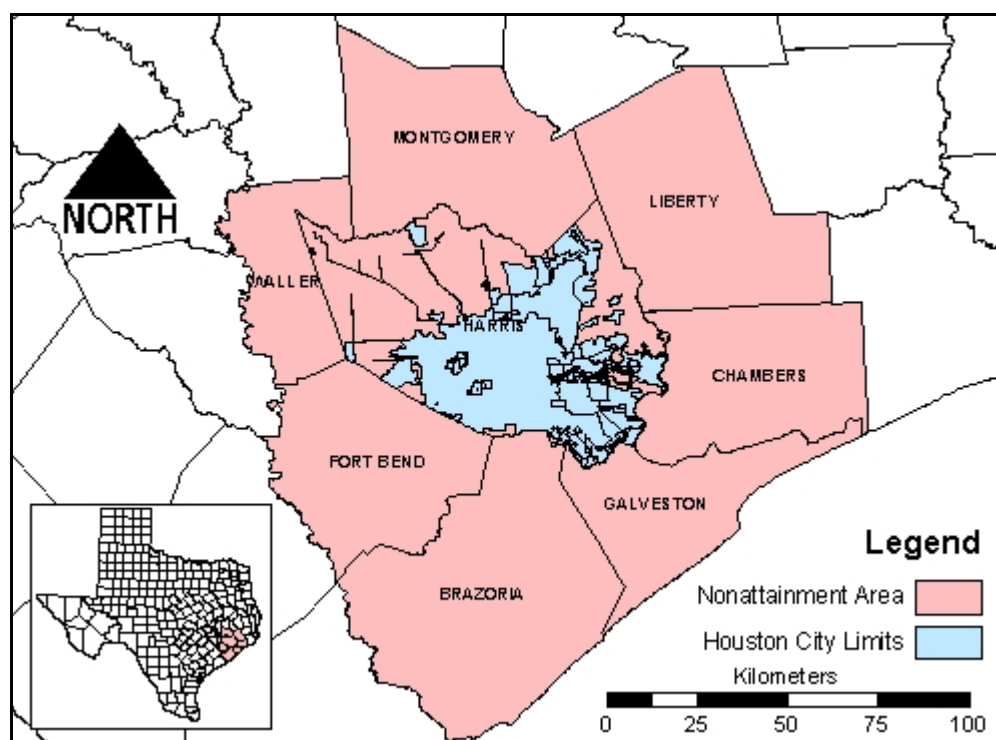
Figure 2.2. The Houston/Galveston Nonattainment Area. It consists of eight Gulf Coast counties. The city of Houston is located in Harris County.

2.3. Residential areas

The residential neighborhoods that are the focus of this study have varying amounts and types of vegetative cover. Although residential areas are generally not as 'hot' as commercial and industrial areas, newer neighborhoods are generally significantly warmer than older neighborhoods that have older (more) tree cover (Aniello et al., 1995). Research has demonstrated that forested areas that were cleared for residential development are "closely related to large increase[s] in surface temperatures" (Lo & Quattrochi, 2003: 1059). However, some newly developed residential neighborhoods endeavor to preserve the older tree canopy while constructing new homes. The Woodlands in the northern Houston Metropolitan Area is one example

of such a development. The average temperatures in The Woodlands are significantly cooler than temperatures located in newly developed neighborhoods that clear the land of vegetation prior to home construction. A Lake Houston neighborhood located east-northeast of downtown Houston is an example of a residential development with approximately the same home density pattern and price values of The Woodlands but exhibits significantly warmer temperatures, due to the development style that it employs. The Woodlands represents a residential area with significant tree canopy, and the Lake Houston neighborhood represents a residential area lacking tree canopy. These two neighborhoods also highlight the contrast in terms of temperature impact between a development style that preserves tree canopy and one that clears vegetation prior to construction.

There are a number of residential neighborhoods in the Houston Metropolitan Area in close proximity to each other that possess the same type of structural characteristics as The Woodlands and the Lake Houston neighborhood. This study analyzes the micro-urban heat island phenomenon and the impact of neighborhood development by focusing on residential areas in proximity to each other that exhibit varying amounts of various types of vegetation cover.

CHAPTER III

APPROACH AND METHODOLOGY

3.1. Overview

The general approach and methodology of the micro-scale vegetation measurement techniques and evaluation of the micro-urban heat island phenomenon in this study are illustrated by the flow chart in Figure 3.1. After rigorous geo-coding of the Landsat ETM+ imagery is accomplished, the thermal channel from the imagery is processed to derive effective at-satellite temperatures. The LIDAR data are processed to obtain feature height information for a region exhibiting a substantial range of vegetation cover abundance and type in the residential areas. By utilizing a 1 meter spatial resolution false color near-infrared aerial photo, an NDVI image with a high spatial resolution is created; the high-resolution NDVI image is then used to create an NDVI mask through a thresholding process, which defines vegetation coverage. A stratified random sampling technique is used to obtain 442 purely residential sample areas possessing different structural characteristics in regard to vegetation cover. By masking the processed LIDAR feature height data with the high-resolution NDVI mask, tree canopy and low-level vegetation (grass and low-lying plants) are quantified for each sample area. Descriptive statistics are obtained for the sample areas, and correlation and regression statistical methods are used to analyze the relationships between the micro-urban heat island effect and residential-structure. This chapter details the data, methodology, and techniques employed for the micro-scale study that are highlighted in

Figure 3.1 and the processing steps of the larger spatial-scale analysis that is used to evaluate the effectiveness of the micro-scale vegetation measurement approach.
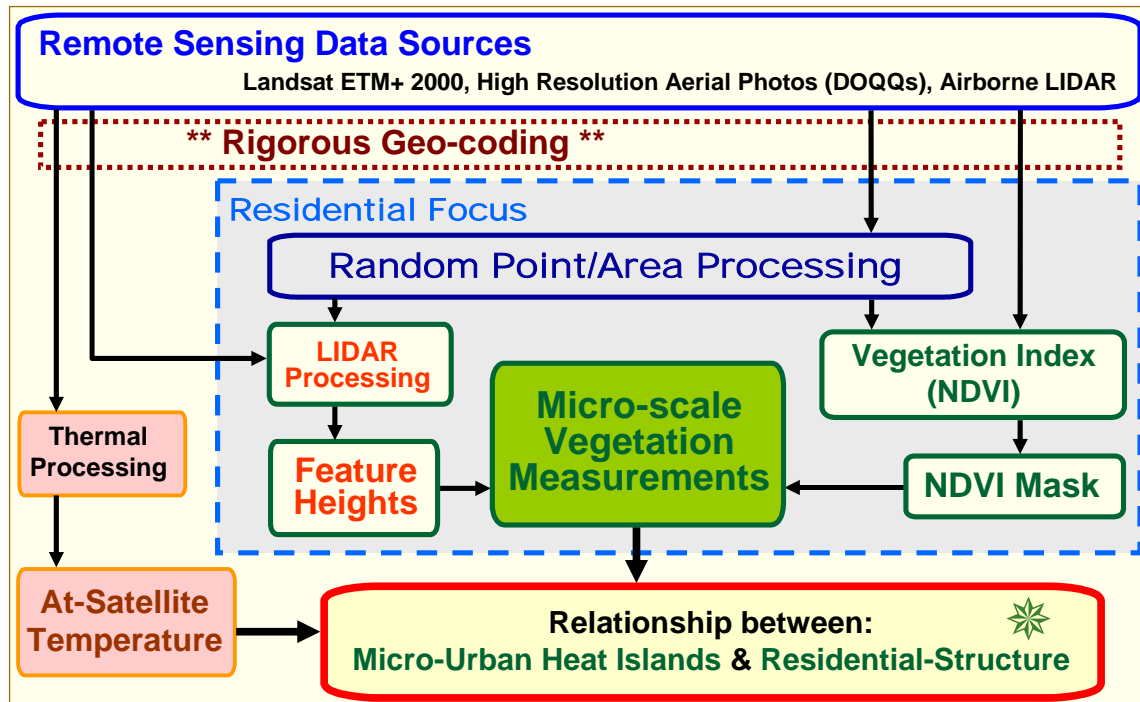
Figure 3.1. Approach and methodology flow chart. The flow chart broadly depicts the various processing steps taken in this study.

3.2. Data sources

A variety of remote sensing data are used in this study. 1) The Landsat ETM+ imagery from the Texas Natural Resource Information System was acquired January 10, 2000 with a thermal band (10.4-12.5μm) at a spatial resolution of 60 meters. 2) Two sets of aerial photographs or DOQQs (Digital Orthophoto Quarter Quadrangles) are utilized. The 1995 DOQQs from the Texas Natural Resource Information System are false color near-infrared composites. The 2002 natural color DOQQs from the Houston-Galveston

Area Council have a spatial resolution of 0.3048 meters (1 foot). 3) The 2001 Airborne

LIDAR data from the Harris County Flood Control District and TerraPoint, LLC

employed in this research have a horizontal accuracy of about 1.5 meters and a vertical

accuracy of approximately 15 centimeters (Campbell, 2002; Krabill et al., 1984). Table

3.1 provides detailed information about each of the data sources utilized in this study.

Table 3.1
Data Source Descriptions

Data Type	Band	Spectral Resolution (μm)	Band Description	Spatial Resolution (m)	Acquisition Date
Landsat 7 ETM+	1	0.450 - 0.515	blue	30	January 10, 2000
	2	0.525 - 0.605	green	30	
	3	0.630 - 0.690	red	30	
	4	0.750 - 0.900	near-infrared	30	
	5	1.55 - 1.75	middle-infrared	30	
	6	10.40 - 12.50	thermal-infrared	60	
	7	2.08 - 2.35	middle-infrared	30	
	8	0.52 - 0.90	panchromatic	15	
1995 DOQQs	1	0.55	green	1.0	January 23, 1995
	2	0.65	red	1.0	
	3	1.00	near-infrared	1.0	
2002 DOQQs	1	0.45	blue	0.3048	January 2002
	2	0.55	green	0.3048	
	3	0.65	red	0.3048	
Airborne LIDAR	1		Bare Earth DEM	4.572	November 2001
	2		Feature Elevations	1.524	

The 2002 DOQQs used in this research have provided detailed information about

the residential study areas. The high-resolution of this aerial imagery has proven to be

extremely valuable in identifying the multiple land-cover types present in the residential

land-use classes. Residential land-use consists of homes, lawns, low-lying plants, trees,

concrete, streets, and even pools. These various land-use types define the residential-

structure of neighborhoods. Figure 3.2 illustrates the variety of land-cover type that can

be found in a residential neighborhood.

Figure 3.2. Example of the high-resolution 2002 DOQQ. This clip of the 1 foot resolution aerial photography illustrates the level of detail that can be examined in residential areas. Many different types of land-cover can be identified.

3.3. Geo-coding satellite imagery

Rigorous geo-coding of the 2000 Landsat ETM+ data using high-resolution

DOQQ imagery as a control has provided sub-pixel level accuracy. Geo-coding of the

Landsat data was performed using an affine transformation (first-order polynomial) and

41 Ground Control Points (GCPs), which are common fixed features that are identifiable

on both the Landsat imagery and the aerial photographs (Lillesand et al., 2004;

Campbell, 2002). The Root-Mean-Squared (RMS) error for the GCPs is calculated to provide an accuracy measure for the geo-coding process (Campbell, 2002; Hellwich & Ebner, 2000). ESRI ArcGIS software was utilized during the geo-coding process; Figure 3.3 displays the software interface and the locations of the 41 GCPs used in the process. The 2000 Landsat ETM+ data, as received, was misaligned with the DOQQ imagery by approximately 130 meters. After rigorous geo-coding, the RMS error was reduced to only 9.77 meters. Considering the Landsat panchromatic band has a spatial resolution of 15 meters, the geo-coding process has transformed the imagery to sub-pixel level accuracy. This higher level of accuracy is absolutely necessary for research at this detailed, micro-level that focuses on the differences in vegetation and development structure between residential neighborhoods in close proximity.
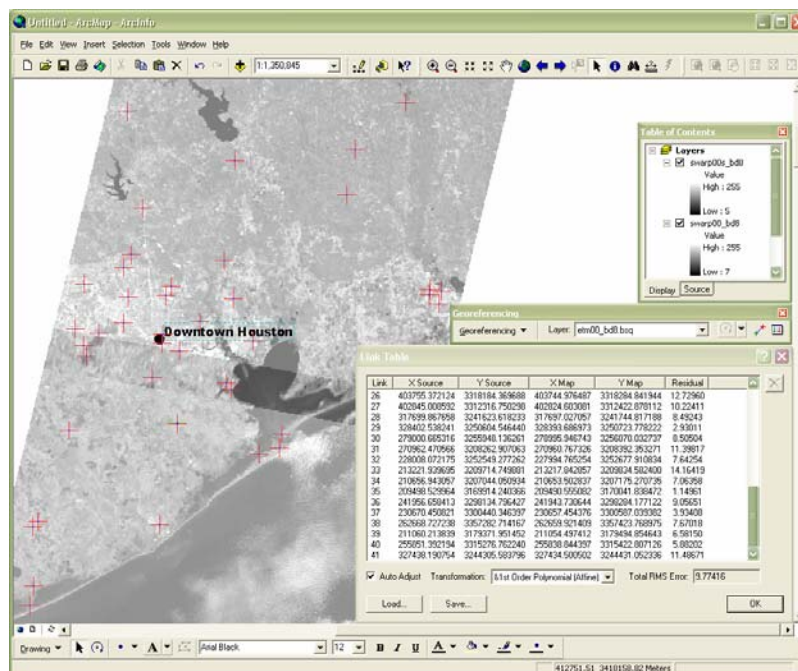
Figure 3.3. ESRI ArcGIS geo-coding interface. The crosshairs mark the locations of the 41 GCPs used to geo-code the 2000 Landsat ETM+ data. A sub-pixel RMS error of 9.77 meters was achieved.

3.4. Derivation of the spatial distribution of surface temperature

Some of the short-wavelength energy radiated from the Sun is transformed by surface materials and emitted back into the atmosphere as long-wavelength energy (Jensen, 2000). Differences in the magnitude of emitted thermal energy from various land-cover types can affect the "density, dynamics, and importance of other energy fluxes linked to specific landscape characteristics" (Quattrochi & Luvall, 2004: 2). Thermal sensors record the energy emitted from the Earth's surface. The thermal band of the 2000 Landsat ETM+ data has a spatial resolution of 60 meters and records emitted electromagnetic energy from the Earth's surface between the spectral wavelengths of 10.4 and 12.5µm. Landsat ETM+ imagery is widely available and has a relatively high spatial resolution for the thermal band compared to other commonly utilized satellite-based thermal sensors. Therefore, these data provide important information regarding the general patterns and spatial distribution of temperature variation for residential areas.

In this study, the digital number values from the thermal band of the 2000 Landsat ETM+ data are converted to effective at-satellite temperatures through two simple processing steps. First, the digital number (DN) of the thermal band is converted into radiance values (L) using the following simplified equation:

$$L = L_{min} + (L_{max} - L_{min}) * DN / DN_{max} \tag{3.1}$$

where L_{max} and L_{min} are published constant coefficients (17.04 and 0.0 respectively) for thermal band 6 of the 2000 Landsat ETM+ data, DN is the quantized calibrated pixel value of each 60x60 meter pixel in the image, and DN_{max} is equal to 255, which is the maximum quantized calibrated pixel value for the image (NASA, 2004). Second, the

radiance values (L) are converted to effective at-satellite brightness temperatures (T_b) in Kelvin, which is a more physically useful variable, by using the inverse of Planck's equation of radiation:

$$T_b = \frac{K_2}{\ln\left(\dfrac{K_1}{L} + 1\right)} \tag{3.2}$$

where K_1 and K_2 are calibration constants, 666.09 and 1282.71 respectively, under an assumption of unity emissivity (NASA, 2004; Aniello et al., 1995). Remotely sensed effective at-satellite brightness temperature measurements require the use of *in situ* ground truth data and/or radiosonde data to calibrate for typical emissivity values of common surface materials (Schmugge et al., 2002; Francois & Ottle, 1996; Vidal, 1991; Henry et al., 1989). With the emissivity values, the effective at-satellite temperatures (T_b) can be converted into physical surface temperatures (Lo & Quattrochi, 2003).

However, research has demonstrated that the differences between the effective at-satellite brightness temperatures and the emissivity-corrected physical surface temperatures to be "very small" (Lo & Quattrochi, 2003: 1058; Nichol, 1996). In addition, this study is interested in the relative temperature differences between neighborhoods in geographic proximity to one another. Therefore, the effective at-satellite temperatures are adequate, and it is not necessary to calculate the actual physical surface temperatures (Aniello et al., 1995). The thermal band data from 2000 Landsat ETM+ imagery utilized in this study are processed to effective at-satellite temperatures in terms of Kelvin. Figure 3.4 illustrates the urban heat island effect by displaying the

processed thermal data for a part of the Houston Metropolitan Area, which overlays a

natural color composite created from the 2000 Landsat ETM+ imagery.
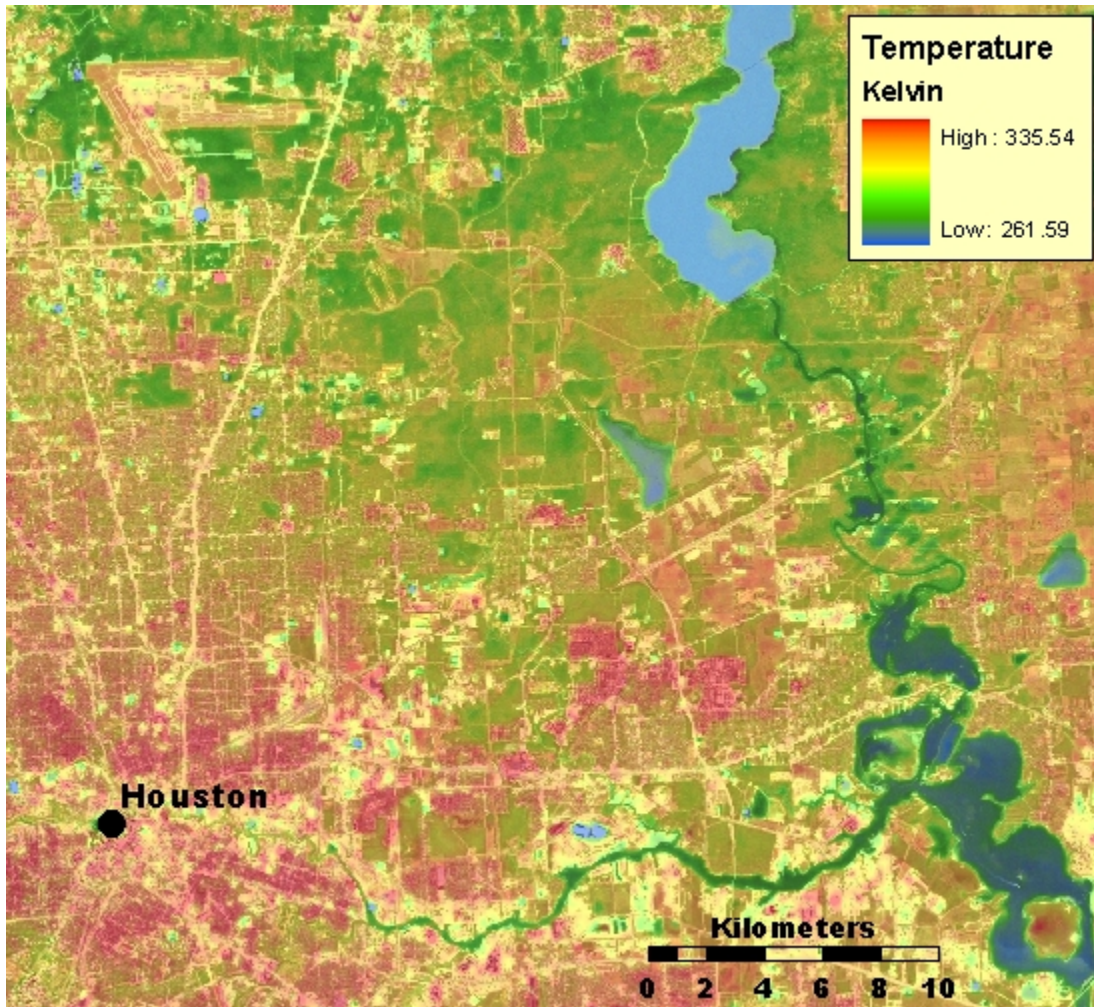
Figure 3.4. Processed 2000 Landsat ETM+ thermal band. This image illustrates the general thermal characteristics of part of the Houston Metropolitan Area. The thermal band overlays a natural color composite of the 2000 Landsat ETM+ imagery.

3.5. Classification of land-use and land-cover

The term 'land-cover' is associated with the form or materials covering the land

surface: forest, water, homes, crops, asphalt, etc. 'Land-use' refers to the functional use

of the land surface: agriculture, commerce, residential, etc. Many different land-cover types can be present in one land-use type (Jensen, 2005). When utilizing a supervised classification scheme, the land-use and land-cover dynamics must be taken into account in order to manually select training sites for the classification algorithm. The training sites selected in this study represent classes in accordance with the USGS Land-use/Land-cover Classification System, Level I and Level II with some modification (Campbell, 2002; Jensen, 2000). As the interest of this study is residential neighborhoods with variable amounts and types of vegetation cover, the traditional residential classification has been divided into residential areas that exhibit significant abundance of tree canopy and residential areas lacking tree canopy. Utilizing natural color and false color near-infrared composites derived from the 2000 Landsat ETM+ imagery and the 1995 and 2002 DOQQs as references, 177 training sites representing 7 land-cover types were delineated (Lillesand et al., 2004; Lo et al., 1997). The classes used in this study are urban, agricultural, forest, water, barren land, residential with trees, and residential without trees.

Based on the visible and infrared bands (bands 1-5, and 7) of the 2000 Landsat ETM+ imagery (30 meter spatial resolution), a supervised maximum likelihood classification was adopted to create a Land-use/Land-cover (LULC) map. The decision rule utilized by the maximum likelihood classification scheme is based on probability and assumes a normal distribution for the statistics of each class in each band (Jensen, 2005). Each pixel in the image is assigned to a class according to the highest probability (maximum likelihood) that it belongs to that class (Jensen, 2005). The larger spatial-

structure of the urban heat island of Houston has been analyzed in association with LULC types and vegetation to evaluate the micro-scale vegetation measurement approach as a better surrogate for explaining surface temperatures for residential neighborhoods, which is the focus of this thesis.

An accuracy assessment using 100 stratified random points, high-resolution DOQQs, and knowledge of the Houston Metropolitan Area was performed. Each of the stratified random points was examined in relation to the classification image and the LULC ground-truth. The confusion matrix (Table 3.2) reveals the overall classification accuracy to be 83 percent and the kappa coefficient to be 0.77956. The kappa coefficient is a measure of accuracy between the 100 randomly selected ground true points and the classification map derived from the remote sensing data. A kappa coefficient that is greater than 0.80 represents a strong agreement (Jensen, 2005; Campbell, 2002). The accuracy of individual categories can be measured in two ways: the producer's accuracy is a measure of omission error for each class; the user's accuracy is a measure of commission error or reliability (Jensen, 2005). The commission error for both the residential with tree canopy class and the residential without tree canopy class are relatively low. Although the classification results display some problems, the classification image is used as merely a reference for the micro-scale vegetation measurement analysis focused on residential-structure.

Table 3.2
Confusion Matrix for Maximum Likelihood Classification

	Class	Urban	Agricultural	Forest	Water	Barren	Res w/tree	Res w/o	Total
Maximum Likelihood Classification	Urban	7	0	0	0	3	0	1	11
	Agricultural	0	17	0	0	4	0	0	21
	Forest	0	3	36	0	1	1	0	41
	Water	0	0	0	7	1	0	0	8
	Barren	0	0	1	0	4	0	1	6
	Residential w/ Trees	0	0	1	0	0	7	0	8
	Residental w/o Trees	0	0	0	0	0	0	5	5
	Total	7	20	38	7	13	8	7	100

(Ground Truth (Number of Pixels) spans the Urban through Res w/o columns)

Overall Accuracy = (83/100) 83.0%
Kappa Coefficient = 0.77956

	Error	Producer's Accuracy		Omission	User's Accuracy		Commission
Maximum Likelihood Classification	Class	(Pixels)	(Percent)	(Percent)	(Pixels)	(Percent)	(Percent)
	Urban	7/7	100.0	0.0	7/11	63.6	36.4
	Agricultural	17/20	85.0	15.0	17/21	81.0	19.0
	Forest	36/38	94.7	5.3	36/41	87.8	12.2
	Water	7/7	100.0	0.0	7/8	87.5	12.5
	Barren	4/13	30.8	69.2	4/6	66.7	33.3
	Residential w/ Trees	7/8	87.5	12.5	7/8	87.5	12.5
	Residental w/o Trees	5/7	71.4	28.6	5/5	100	0.0

Figure 3.5A is a high-resolution (1 foot) aerial photograph from 2002. Region A lacks tree canopy, and Region B has a significant amount of tree canopy. Figure 3.5B illustrates classification results that have been smoothed using a 3x3 neighborhood majority function. The yellow pixels represent residential areas lacking tree canopy, and the light green pixels represent residential areas with significant tree canopy. The red pixels signify urban areas and the dark green pixels are forested areas. Analysis suggests that the classification of residential areas in regards to amount of tree canopy is effective. The delineated regions indicate areas where a detailed analysis was conducted using temperature, an NDVI, and feature heights from LIDAR data. The distance from the center of Region A to the center of Region B is only 1,200 meters. This proximity

essentially controls the climatic variables that exist over greater distances. Although the two neighborhoods are in close proximity to each other, their vegetation cover, as perceived through remote sensing and the classification algorithm, varies greatly.
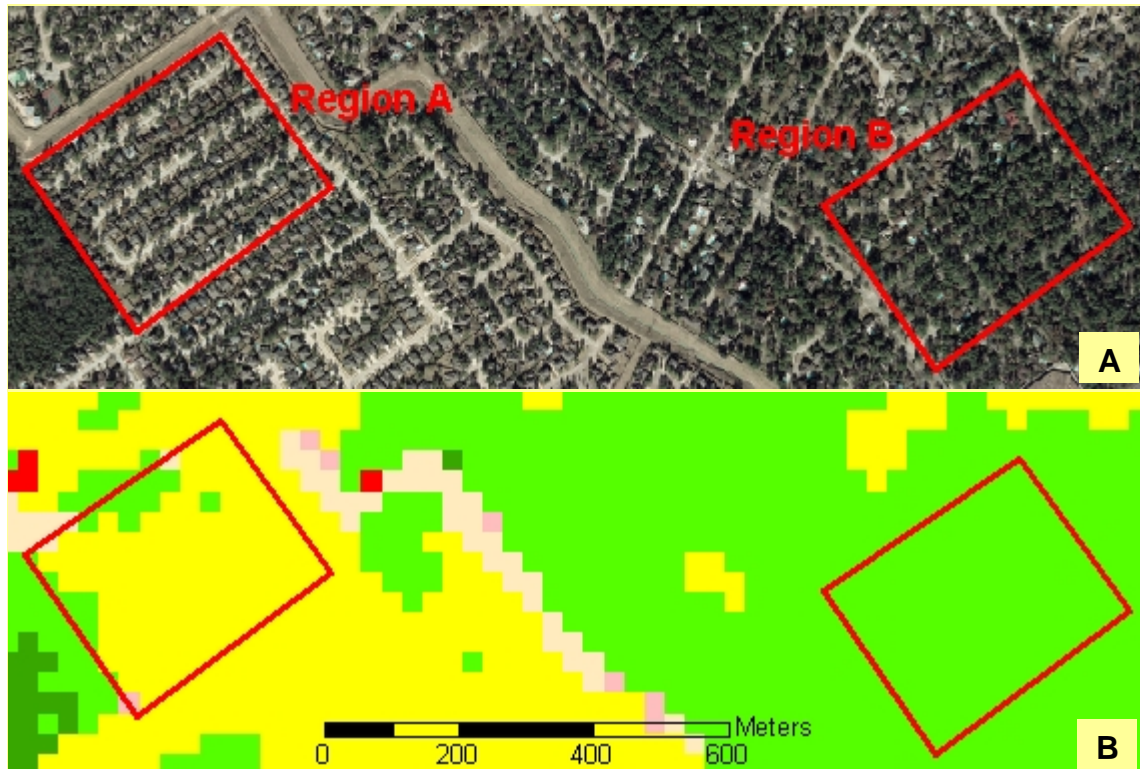
Figure 3.5. Proximal residential areas classified based on vegetation. These regions represent residential areas with significant differences in abundance and type of vegetation cover. (A) 2002 aerial photograph. Region A is an area lacking tree canopy and Region B is an area with significant tree canopy. (B) Classification results identifying residential areas lacking tree canopy (yellow) and residential areas with significant tree canopy (green).

Figure 3.6 illustrates the classification results for a portion of the Houston Metropolitan Area. The red urban areas correspond to commercial and industrial uses and transportation networks (roads and airports). The light tan agricultural areas represent crop land, and the dark tan barren land areas represent sand surfaces and

grasslands. The dark green forested areas correspond to surface regions covered with deciduous and coniferous trees. The blue areas represent water. The residential class has been divided into residential areas with significant tree canopy (green) and residential areas lacking tree canopy (yellow).
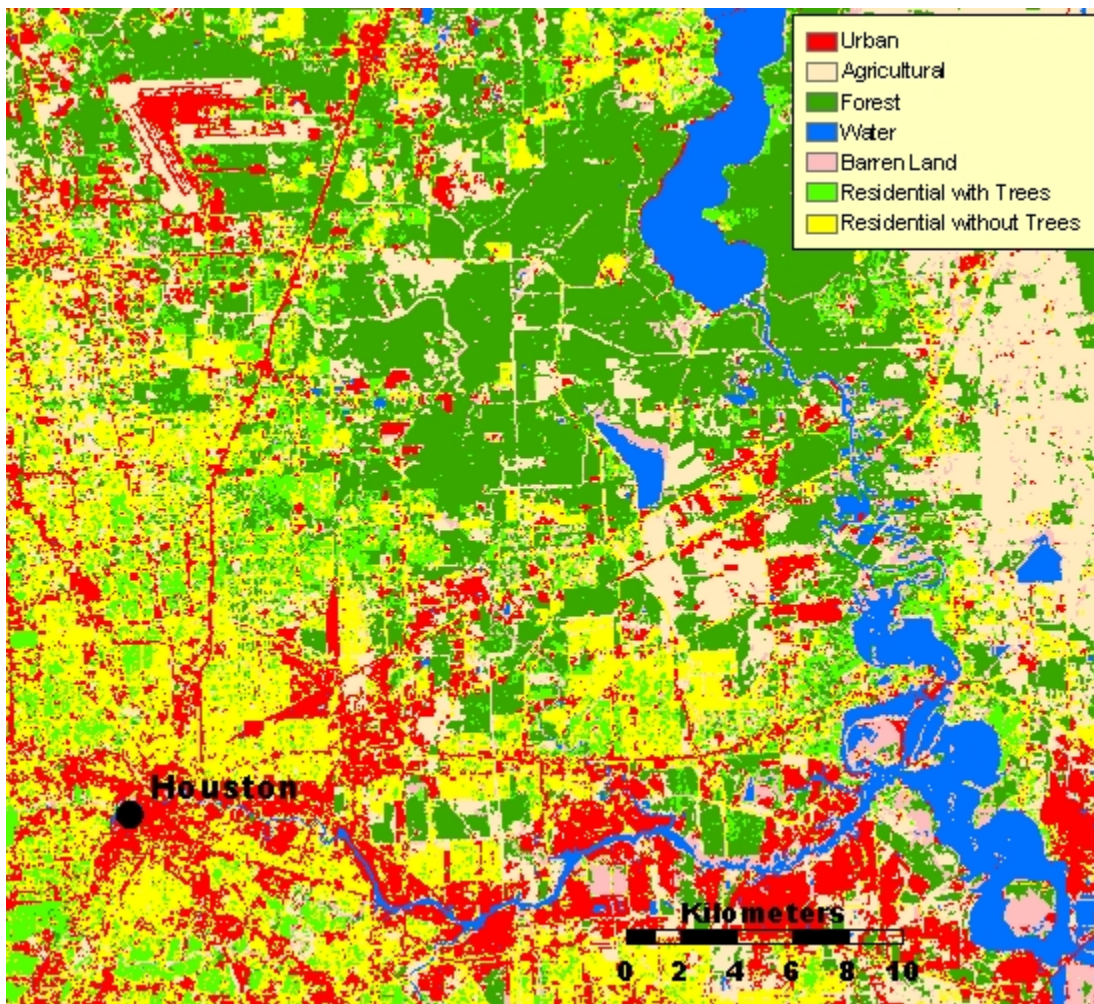
Figure 3.6. Maximum likelihood classification results. The classification scheme was able to divide residential areas according to the level of tree canopy present.

3.6. Derivation of NDVI values and total vegetation cover

The Normalized Difference Vegetation Index (NDVI) is created through a method of band ratioing, and it measures the greenness of the environment and the amount and/or quality of vegetation (Lillesand et al., 2004; Lo & Quattrochi, 2003; Campbell, 2002). This band rationing technique utilizes the fact that red light is absorbed by the chlorophyll and infrared radiation is strongly reflected by the mesophyll tissue in green vegetation, which provides a stark difference in the red and infrared values recorded by the sensor (Campbell, 2002). The relationships between urban heat islands and vegetation coverage have been analyzed by correlating surface temperature with the NDVI (Gallo & Tarpley, 1996). The near-infrared and red bands of the 2000 Landsat ETM+ data and the 1995 false color near-infrared composite DOQQ have been separately used to compute the NDVI with this equation:

$$NDVI = \frac{NearIR - red}{NearIR + red} \tag{3.3}$$

where *NearIR* is the near-infrared band, which is band 4 for the Landsat ETM+ imagery and band 3 for the DOQQ, and *red* is the red band, which is band 3 for the Landsat ETM+ imagery and band 2 for the DOQQ.

Figure 3.7 represents the NDVI image for part of the Houston Metropolitan Area using 2000 Landsat ETM+ data (30 meter spatial resolution). The dark green and green areas represent higher NDVI values and a greater amount of healthy green vegetation; the red in the image represents a lack of vegetation, which corresponds to transportation networks, urban development, and some agricultural fields.
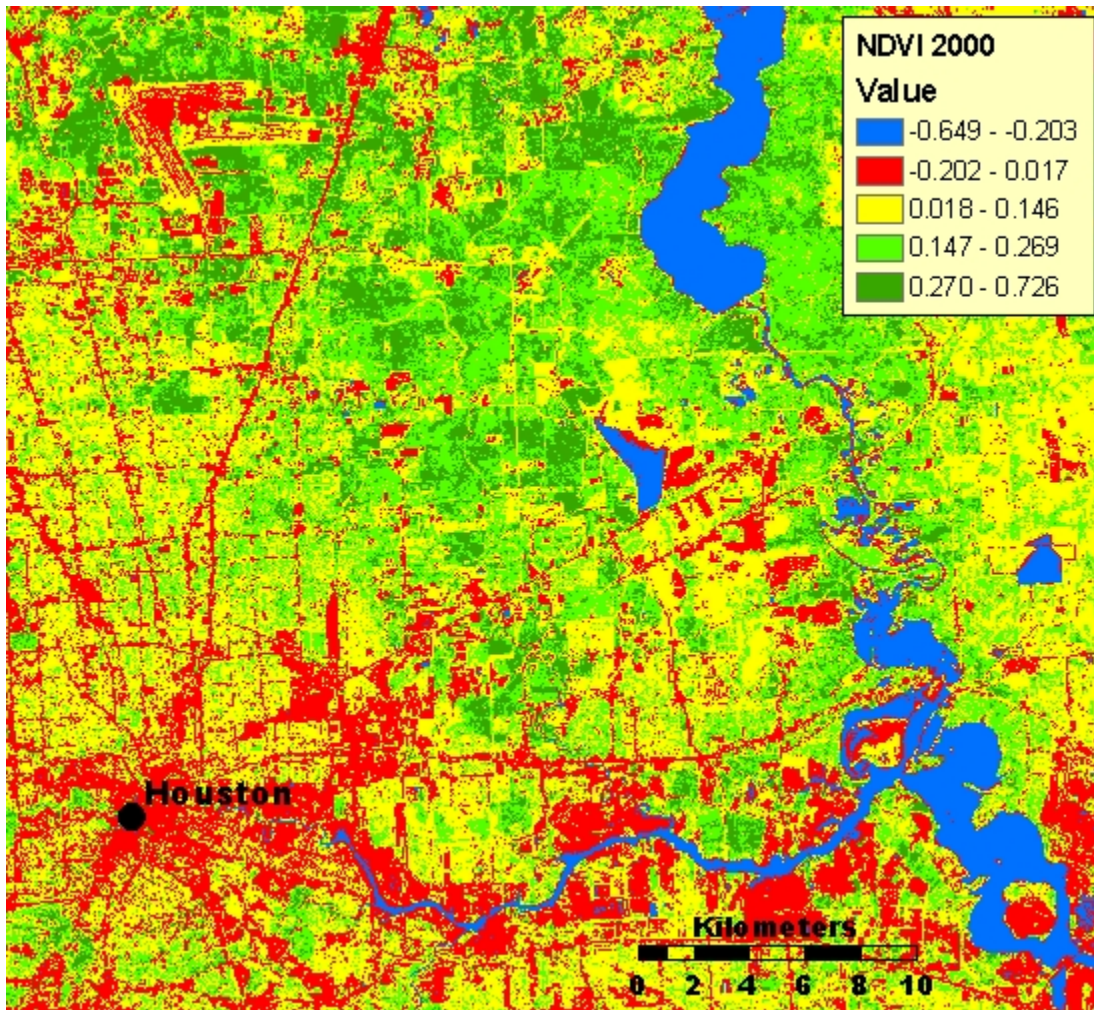
Figure 3.7. NDVI results from 2000 Landsat ETM+ data. This represents part of the Houston Metropolitan Area. The dark green and green areas represent a greater amount of green vegetation; the red represents a lack of vegetation corresponding to transportation networks, urban development, and some agricultural fields; and the blue represents water and an absence of vegetation.

The 1995 false color near-infrared composite DOQQ at 1 meter spatial resolution provides much more detailed results from a geographic perspective. Qualitative analysis of the results from the NDVI band ratioing at the higher spatial resolution was performed through incorporating prior knowledge about the study area and comparing the results to the 1995 and 2002 aerial images. After analysis, it was determined that a

threshold NDVI value of 0.0 divided most vegetative cover from the man-made features (houses, roads, etc.), bare soil, and/or water in the residential study area. The thresholding technique segments the image into two classes (Lillesand et al., 2004). The thresholding technique is utilized to create an NDVI mask, which is illustrated by the partially transparent green layer placed on top of the 1995 DOQQ in Figure 3.8. This NDVI mask layer defines the Total Vegetation Cover measurement for this research. The demarcated area in Figure 3.8 corresponds to region A from Figure 3.5 and represents a residential neighborhood in which the Total Vegetation Cover is made up of mainly low-level vegetation (grass and low-lying plants) and lacks tree canopy. The 1995 NDVI results are combined with feature height information from 2001 LIDAR data in order to derive other micro-scale vegetation measurements.

Figure 3.8. NDVI mask from the 1995 DOQQ. Laid over the 1995 DOQQ, the partially transparent green layer represents the areas with an NDVI value greater than 0.0, which divides the vegetative cover from the man-made features, bare soil, and water. This layer also defines the Total Vegetation Cover for this research. The delineated area corresponds to Region A in Figure 3.5.

3.7. Tall tree canopy extents and heights derived from LIDAR data

LIDAR is an active sensor that uses laser pulses aimed toward the ground, and the time of the pulse return is measured to calculate the distances between the sensor and the various features on or above the ground (Lillesand et al., 2004). "[LIDAR sensors] are unique in being the only sensors that can reliably differentiate between multiple imaged layers" (Campbell, 2002: 239). In other words, LIDAR sensor data can be utilized to obtain bare-Earth information and object height information. The raw LIDAR data consists of a massive number of single return laser measurements corresponding to the ground and feature heights above the ground (e.g., homes, trees, etc.). The raw data, once interpolated, produces a Digital Surface Model (DSM); and if the man-made features are removed, a Digital Canopy Model (DCM) can be created (Nilsson, 1996; Nelson et al., 1988). It is no small process to remove the surface object information (trees, bushes, grasses, buildings, power lines, bridges, etc.) from the LIDAR data to create a bare-Earth DEM, void of tree canopy and man-made structures.

For this research, the raw LIDAR data set and a bare-Earth LIDAR DEM were acquired from the Harris County Flood Control District. The bare-Earth LIDAR DEM was created through processing conducted by TerraPoint, LLC for the Harris County Flood Control District and has a spatial resolution of 15 feet (4.572 meters). In order to obtain the feature height data set for the residential study area, the bare-Earth LIDAR DEM was subtracted from the interpolated raw LIDAR data set (DSM). This is a simple raster calculation and provides the feature heights (*Fh*) relative to the ground for tree canopy and man-made structures for the residential study area (DeMers, 2002; Persson

et al., 2002; Krabill et al., 1984). This map subtraction process can be expressed with the following equation:

$$Fh = Fe - bE \tag{3.4}$$

where Fe is the interpolated feature elevation data set (DSM) and bE is the processed bare-Earth LIDAR DEM; both are relative to sea level. Figure 3.9 graphically illustrates the raster subtraction process: the interpolated DSM (Figure 3.9A) minus the bare-Earth LIDAR DEM (Figure 3.9B) provides the feature heights relative to the ground.
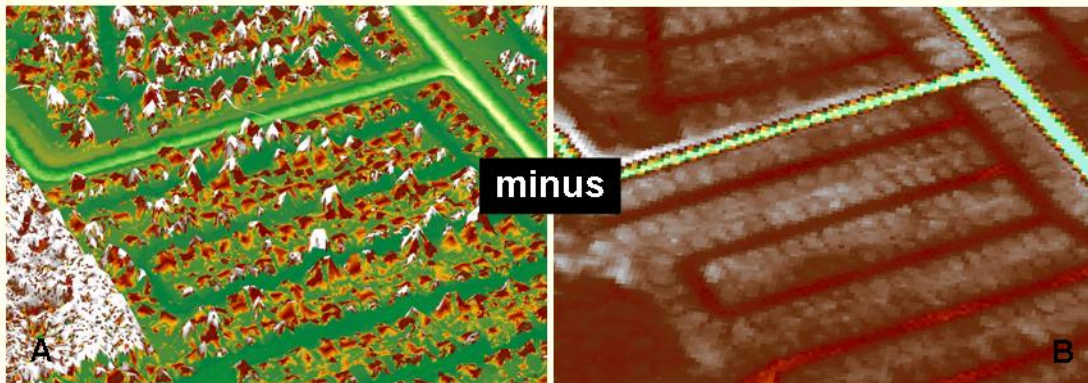
Figure 3.9. Map subtraction of LIDAR data. (A) The DSM or interpolated feature elevation data set. (B) The bare-Earth LIDAR DEM. The bare-Earth DEM is subtracted from the DSM to obtain feature heights.

Qualitative analysis of the feature height LIDAR data set was conducted through incorporating prior knowledge about the study area and comparing the tree heights to the 1995 and 2002 DOQQs. After analysis, it was determined that feature heights $\geq$ 25 feet (7.62 meters) represent the tall tree canopy well while excluding most of the man-made structures (houses) in the residential study area. This thresholding technique provides a measure of the area covered by tall tree canopy in the residential neighborhood. The partially transparent orange layer in Figure 3.10 is laid over a 2002 DOQQ (1 foot

spatial resolution) and represents areas where the tree heights are ≥ 25 feet. This layer defines the Tall Tree Canopy measurement for this research. Figure 3.10 corresponds to region B from Figure 3.5 and represents a residential neighborhood with a significant amount of tree canopy. The 1995 NDVI mask layer is applied to the 2001 feature height LIDAR layer in order to obtain micro-scale measurements of tree canopy and low-level vegetation, which are used to analyze the relationships between residential-structure and micro-urban heat islands in neighborhoods.
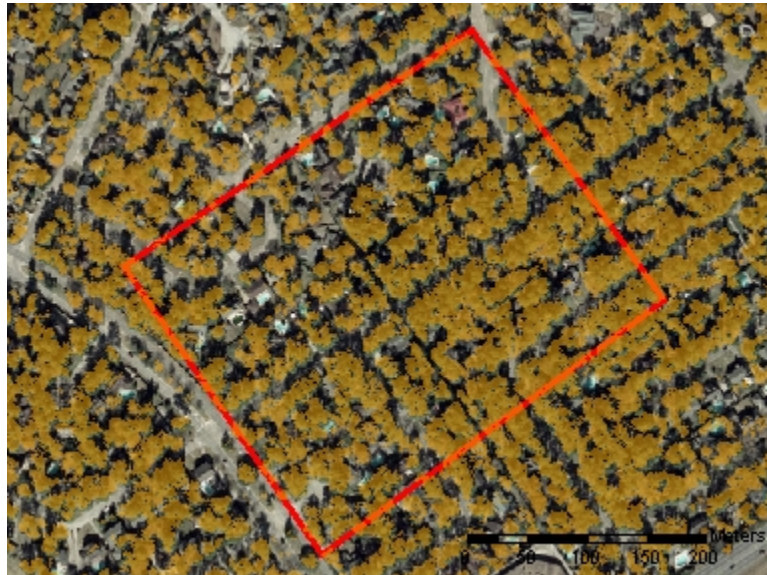
Figure 3.10. LIDAR feature height data. Laid over the 2002 DOQQ, the partially transparent orange layer represents the areas with feature heights equal to or greater than 25 feet, which excludes most of the houses in the residential neighborhood. This layer also defines the Tall Tree Canopy for this research. The delineated area corresponds to Region B in Figure 3.5.

3.8. Derivation of micro-scale vegetation measurements

By utilizing a thresholding technique together with a raster masking process (DeMers, 2002) from the NDVI layer, the man-made structures can be removed from the

LIDAR feature height layer. Therefore, the feature height threshold from the LIDAR data can be lowered to capture the shorter tree canopy along with the Tall Tree Canopy. Figure 3.11 depicts the problem caused by the man-made structures: the red pixels represent LIDAR feature heights between 10 and 25 feet; the brown pixels represent Tall Tree Canopy (feature heights $\geq$ 25 feet). Many of the areas with feature heights between 10 and 25 feet in residential areas represent houses. By utilizing a masking process based on the Total Vegetation Cover (NDVI $>$ 0.0), the houses can be removed from the feature height data set and the tree canopy measurement threshold can be lowered. Figure 3.12 illustrates the results of masking the LIDAR data with the Total Vegetation Cover layer: the green represents the increased area that can be identified as tree canopy.

Adding the additional area identified as tree canopy to the Tall Tree Canopy (already identified through thresholding) created a new micro-scale vegetation measurement. This new layer defines the Total Tree Canopy for this research. Because the sample areas utilized in this research are located in residential areas and most of the man-made features are houses, the amount of error encountered by capturing man-made features heights $\geq$ 25 feet is negligible. However, the amount of tall tree canopy captured by this conditional function is significant.

Section 3.10 lists and describes all of the micro-scale vegetation measurements that are utilized in this research. The micro-scale vegetation measurements are used to quantify residential-structure and provide information about the independent contributions of tree canopy and that of low-level vegetation cover toward lowering residential temperatures.
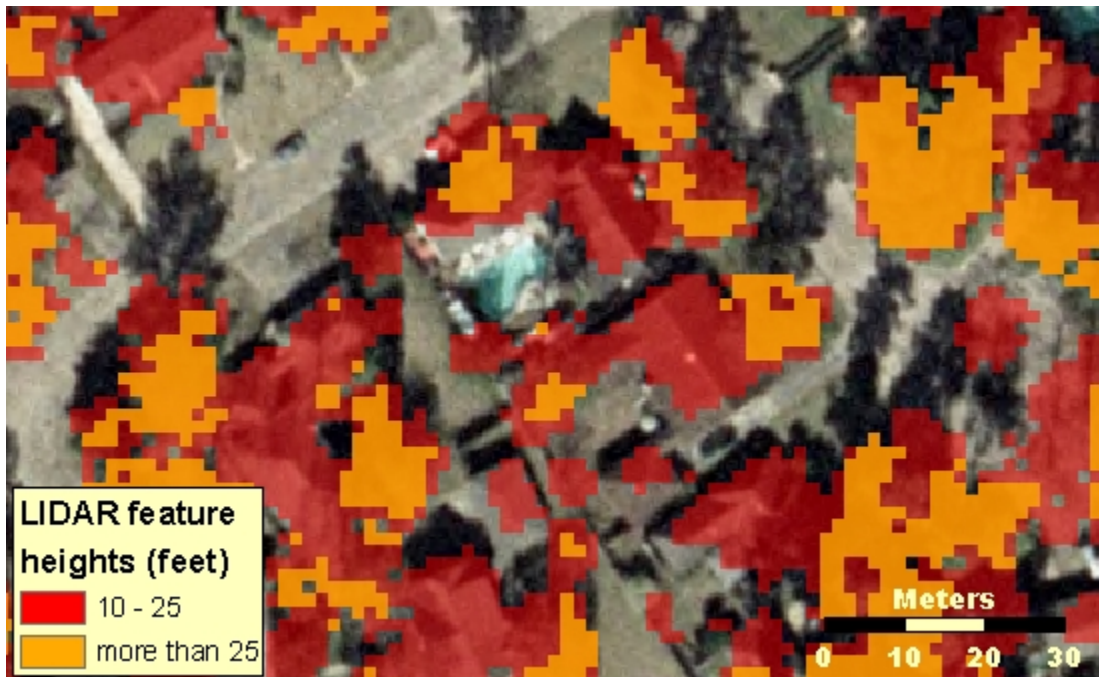
Figure 3.11. LIDAR feature heights without the NDVI mask. Many of the areas with feature heights between 10 and 25 feet represent man-made structures (houses).
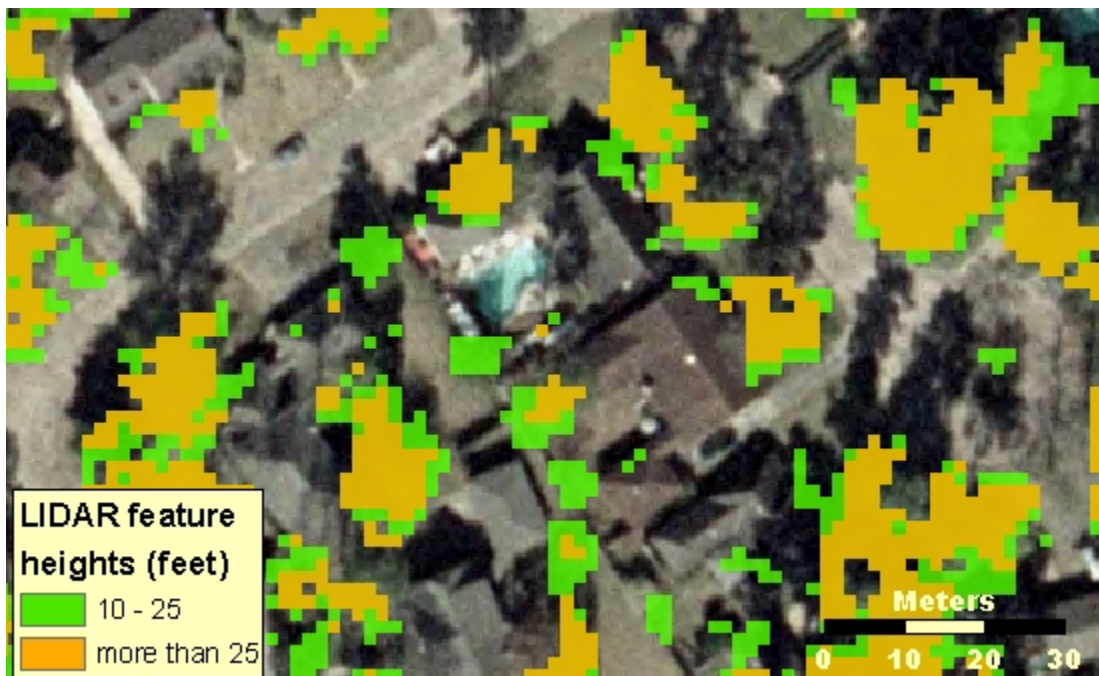
Figure 3.12. LIDAR feature heights with the NDVI mask. The man-made structures (houses) are removed from the feature height data set by the NDVI masking process, and a greater area of tree canopy can be identified by lowering the tree canopy measurement threshold.

3.9. Stratified random residential sample areas

Detailed quantitative analysis is conducted for a larger area that exhibits a residential-structural mix and a wide range of micro-scale measured vegetation abundance and type (Figure 3.13). The mixture of green and yellow pixels in Figure 3.13 represents different amounts of vegetation cover in residential areas. The LULC image was used as a reference; however, the larger study area was selected based upon the large quantity of geographically proximal neighborhoods exhibiting a variety of residential-structures. From this larger area, descriptive statistics of 442 stratified random residential sample areas spread over approximately 46 km^2 are obtained and analyzed in order to quantify the relationships between feature heights, vegetation, and temperature. A GIS is utilized to create a fishnet that functions to: label each of the smaller samples; define the size of each sample; and extract information from each sample. The size of each sample is based partially on the resolution of the thermal data and partially on the characteristics of the larger study area, in terms of observed sizes of contiguous residential neighborhoods. The smaller sample areas were selected based upon a purely residential classification and the absence of change between 1995 and 2001, because the NDVI layer was derived from 1995 imagery and the LIDAR feature heights layer was derived from 2001. The use of temporally correlated NDVI and LIDAR data and/or a highly accurate LULC map could provide a more automated means by which to identify purely residential sample areas.
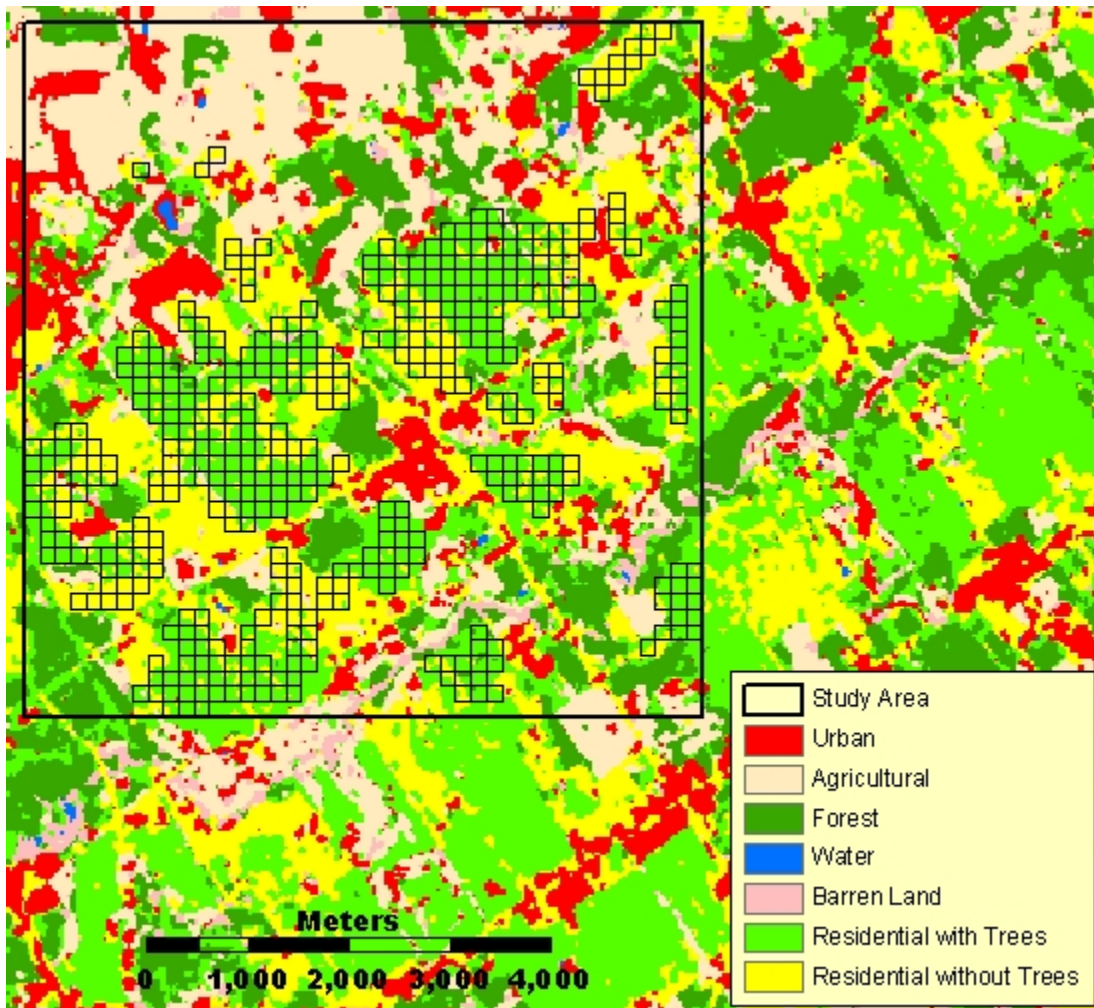
Figure 3.13. Residential study area and classification results. The mixture of green and yellow pixels represents different amounts of vegetation cover for residential areas in proximity to each other. Within the larger study area, 442 smaller stratified random sample areas are demarcated. The samples are spread over a 46km^2 area.

Each sample area is approximately 150x150 meters (more precisely: 23,225.76m^2). Although the samples are spread over an area that is 46km^2, the actual area of all of the samples is about 10.27km^2. Figure 3.14 illustrates the location, density, and size of the 442 stratified random residential sample areas. The percentages of the total area of each residential sample regarding their residential-structural characteristics

are measured. These percentages are evaluated quantitatively using simple linear regression, scatterplots, and multiple regression analysis. The variable values for each sample area are obtained by means of a relatively simple programming function written in C++ program language.
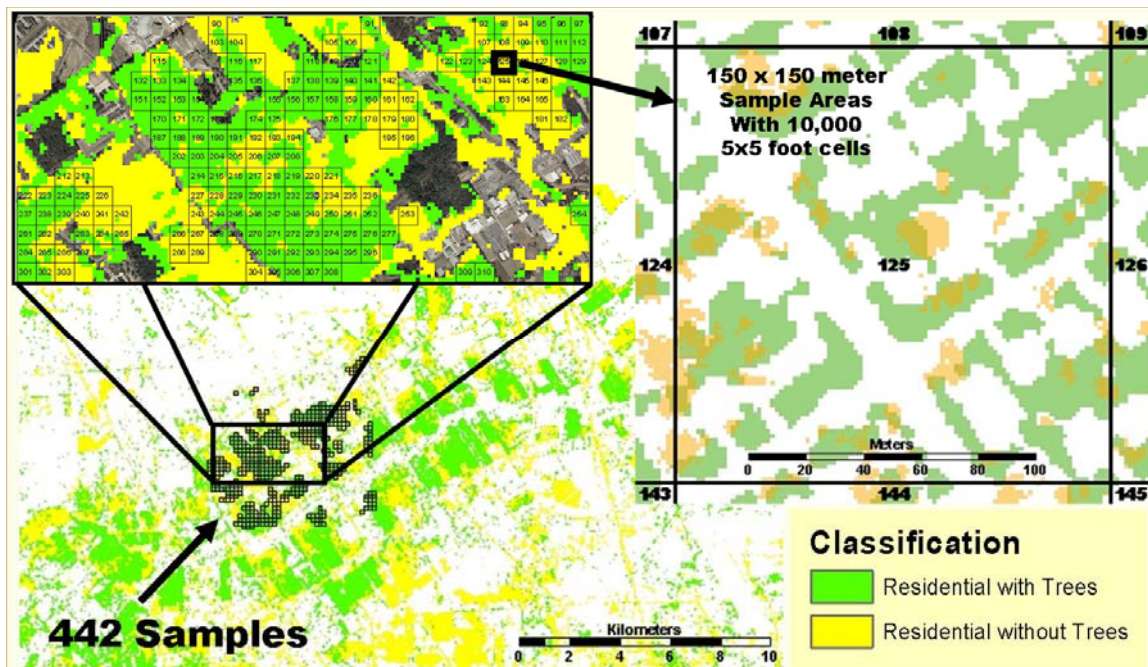
Figure 3.14. 442 stratified random residential sample areas. Each sample area is about 150x150 meters and contains 10,000 5x5 foot cells (1.52x1.52m). The area of all of the samples combined is about 10.27km^2.

The smaller sample areas were selected based upon individual examination to ensure that the area covered within each sample is completely residential and showed little or no change from 1995 to 2002. This was verified by individual examination; comparing the 1995 and 2002 DOQQs, areas that were not purely residential or presented a change of LULC type from 1995 to 2002 were rejected. The gaps in the sample grid displayed in Figure 3.15 are areas where the samples were rejected.
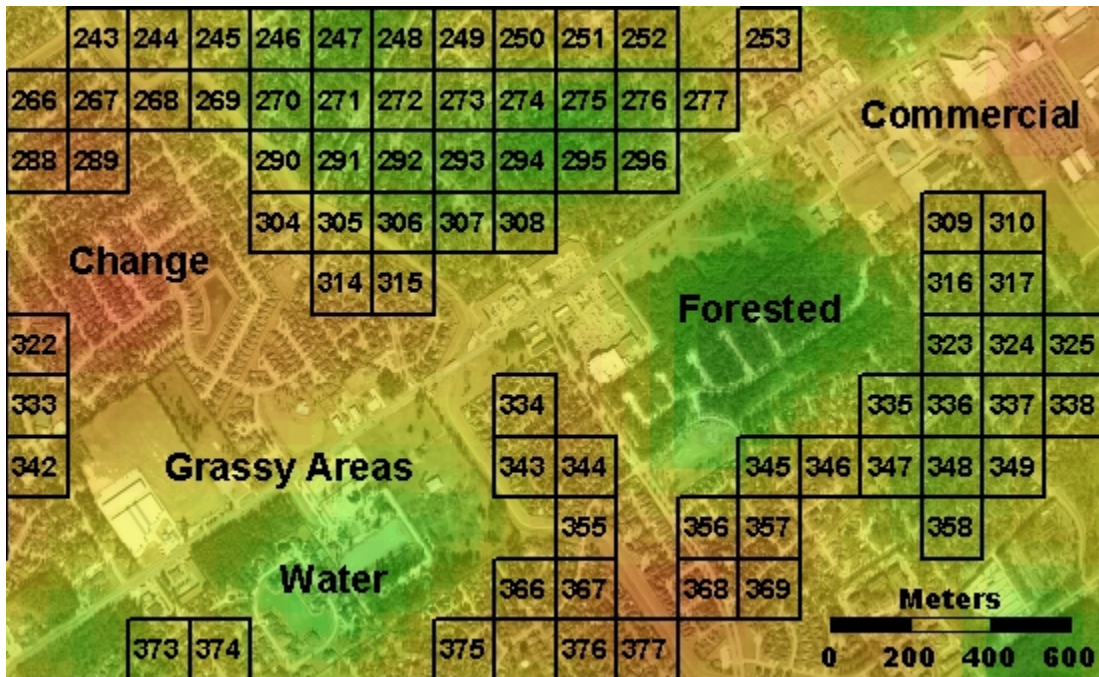
Figure 3.15. Gaps in the residential sample grid. The areas between the numbered samples represent sample areas that were rejected based upon the presence of non residential land-cover or a land-cover change between 1995 and 2002.

3.10. Binary grids representing residential-structure measurements

All of the imagery has been resampled to a cell size of 5x5 feet in order to facilitate direct comparisons to the stratified random residential samples. The following conditional statements are utilized to create the binary grids, which are used to derive and define residential-structure measurements for each residential sample area:

1) Every 5x5 foot cell with an NDVI value > 0.0 are given a value of one and NDVI values ≤ 0.0 are given a value of zero (Total Vegetation Cover);

2) Cells with a feature height ≥ 10 feet are given a value of one and heights < 10 feet are given a value of zero (Above Ground Features);

3) Cells with an NDVI value > 0.0 *and* a feature height ≥ 10 feet are given a value of one and all others are given a value of zero (High NDVI Tree Canopy);

4) Cells with a feature height ≥ 25 feet are given a value of one and heights < 25 feet are given a value of zero (Tall Tree Canopy);

5) Cells with an NDVI value > 0.0 *and* a feature height ≥ 10 feet *or* a feature height ≥ 25 feet are given a value of one and all others are given a value of zero (Total Tree Canopy); and

6) Cells with an NDVI value > 0.0 *and* a feature height < 10 feet are given a value of one and all others are given a value of zero (Low-Level Vegetation).

The percentage values of the area covered by each of these micro-scale vegetation measurements are obtained by means of a relatively simple programming function. These values, the mean NDVI values from the 1995 DOQQ, the mean NDVI values from the 2000 Landsat ETM+ imagery, and the mean feature height value within each sample area is compared to the corresponding mean at-satellite temperature from the thermal data of the 2000 Landsat ETM+ imagery. These descriptive statistics are used to examine the relationships between residential-structure and the micro-urban heat island effect. Through quantitative analysis, simple linear and multivariate regression models are used to explain the level of contribution that each micro-scale vegetation measurement based on abundance and type has toward temperature.

Using sample #125 as an example, the following Figures illustrate the acquisition of the micro-scale vegetation measurements in terms of percentage of total sample area, which are utilized to quantify the influence of residential-structure on temperature.

- Figure 3.16 displays the Total Vegetation Cover: 38.73%.

- Figure 3.17 displays the Above Ground Features: 37.12%, which represent tree canopy and man-made structures (houses).

- Figure 3.18 displays the High NDVI Tree Canopy: 15.33%. 21.79% of the total area is removed, which represents man-made structures and some tall tree canopy with relatively low NDVI values.

- Figure 3.19 displays the Total Tree Canopy: 20.44%. 5.11% of the area, which represents tree canopy with relatively low NDVI values, is added back.

- Figure 3.20 displays the Low-Level Vegetation: 23.40%. From the Total Vegetation Cover layer, 15.33% is removed, which represents High NDVI Tree Canopy.
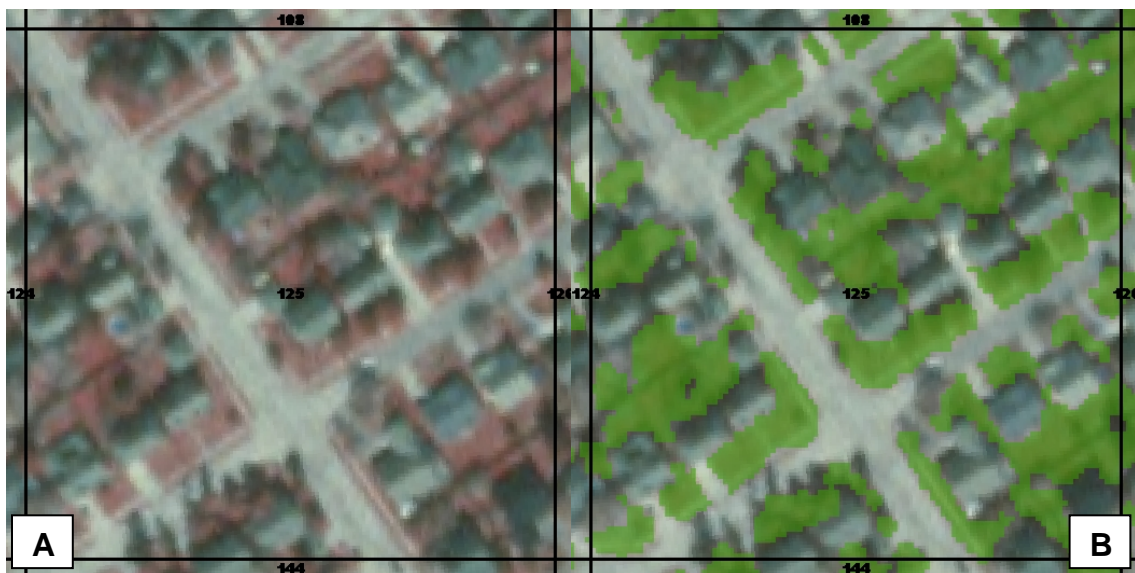
Figure 3.16. Creation of the Total Vegetation Cover layer. (A) 1995 false color near-infrared composite DOQQ used to derive the NDVI has been resampled to a cell size of 5x5 feet. (B) The partially transparent green areas represent cells exhibiting NDVI values > 0.0: 38.73% of the total area.
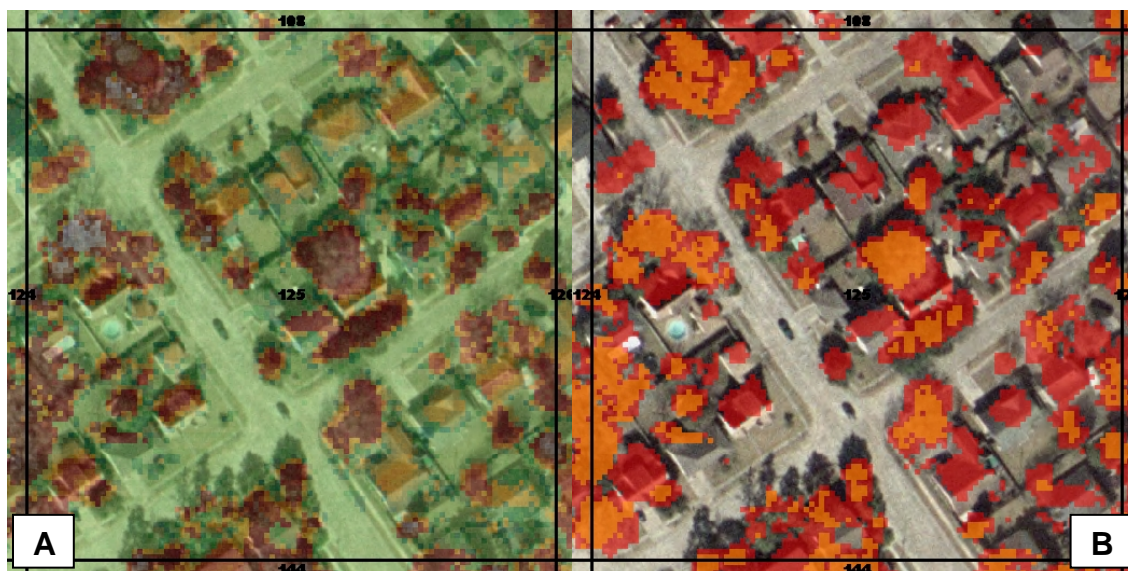
Figure 3.17. LIDAR data and Above Ground Features. (A) LIDAR data processed to provide above-ground feature heights and mean feature height values for each sample. (B) The orange areas indicate feature heights ≥ 25 feet. The partially transparent red areas indicate feature heights ≥ 10 feet, which represents 37.12% of the total sample area.
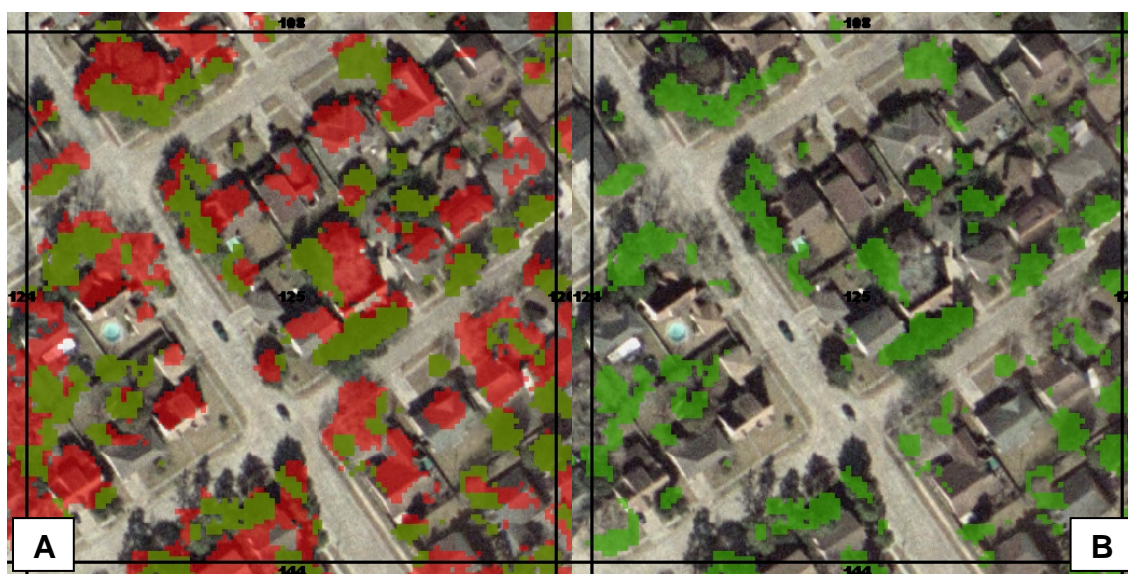
Figure 3.18. Creation of High NDVI Tree Canopy layer. (A) The partially transparent green areas represent 15.33% of the total area and have NDVI values > 0.0 *and* feature heights ≥ 10 feet. The partially transparent red areas correspond to areas with feature heights ≥ 10 feet but NDVI values ≤ 0.0. This is 21.79% of the total area, which is removed. (B) The partially transparent green areas represent High NDVI Tree Canopy, which is 15.33% of the total area.
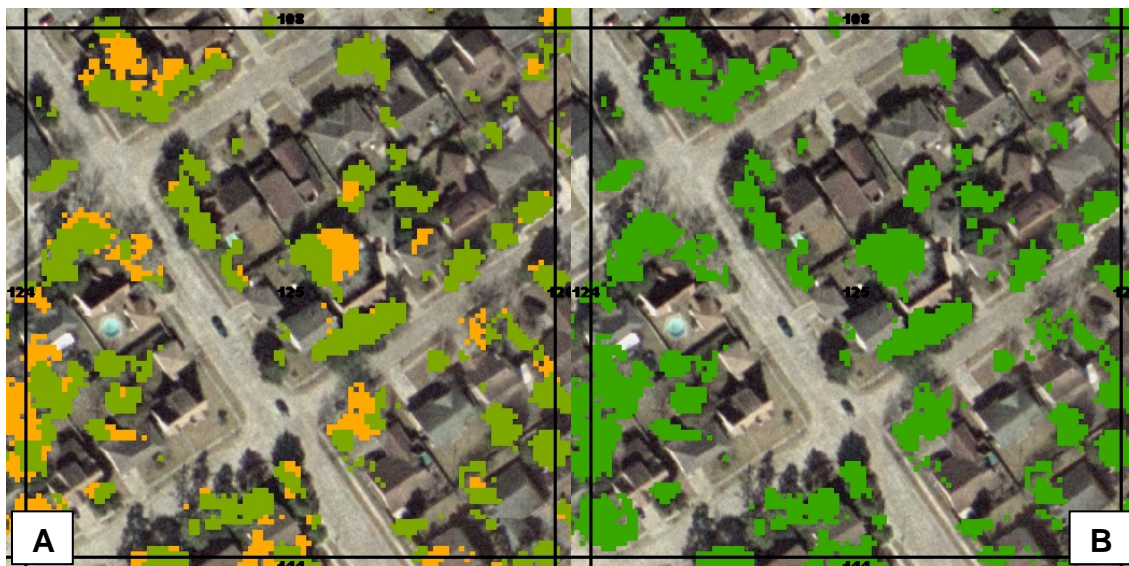
Figure 3.19. Creation of Tall Tree Canopy layer. (A) The green areas are High NDVI Tree Canopy, which is 15.33% of the total area. The orange areas represent tall tree canopy with low NDVI values; these have feature heights $\geq$ 25 feet but NDVI values $\leq$ 0.0, which is 5.11% of the area. (B) The areas of tall tree canopy with low NDVI values are added back to yield Total Tree Canopy, which is 20.44% of the area.
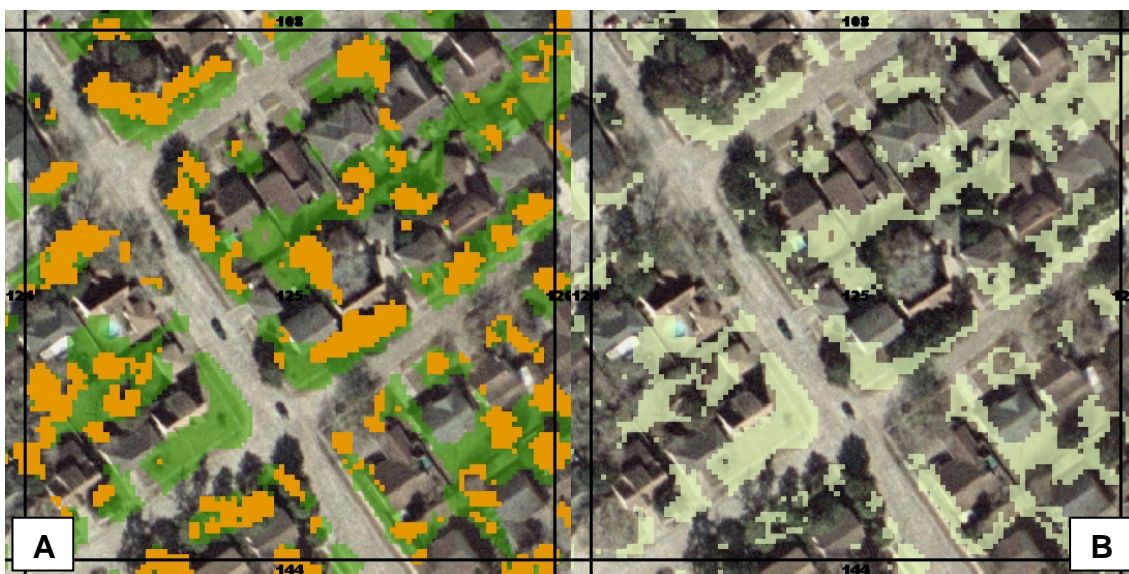
Figure 3.20. Creation of Low-Level Vegetation layer. (A) The partially transparent green areas represent Total Vegetation Cover, which is 38.73%. The orange areas represent High NDVI Tree Canopy, which is 15.33% of the area. (B) The partially transparent light green areas represent Low-Level Vegetation, which is now 23.40%. The High NDVI Tree Canopy, representing 15.33% has been removed.

The thermal data from the 2000 Landsat ETM+ imagery (60 meter spatial resolution) has been resampled to a cell size of 5x5 feet in order to directly compare it to the various binary grids representing different residential-structure characteristics. Figure 3.21A displays the thermal data. The size of the stratified random residential sample areas was partially determined based on the spatial resolution of the thermal data. At a sample area size of approximately 150x150 meters, each sample has a mean at-satellite temperature based upon segments of at least 9 different thermal cells. This procedure helps eliminate outliers in the quantitative statistical analysis of the 442 sample areas and captures the residential thermal patterns. The mean 1995 and 2000 NDVI values for each sample are also evaluated against temperature. The 2000 Landsat ETM+ NDVI image (30 meter spatial resolution) was resampled to a cell size of 5x5 feet (Figure 3.21B).
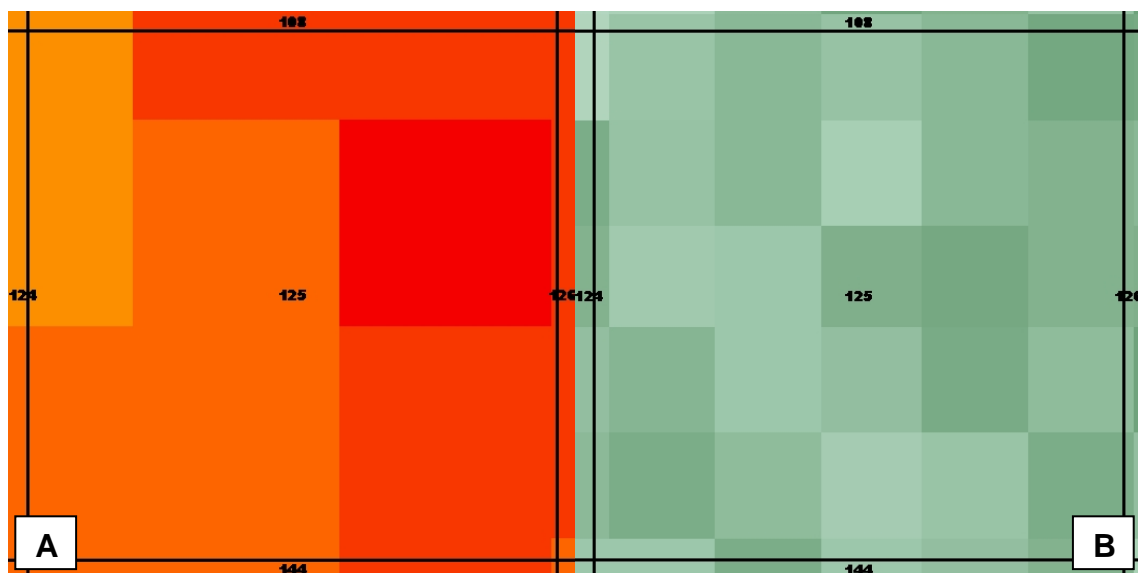
Figure 3.21. Resampled thermal data and NDVI from 2000 Landsat ETM+ imagery. (A) The 2000 thermal data has been resampled to facilitate a direct comparison between the grids. Each sample area size of about 150x150 meters ensures that at least segments of 9 different thermal cells will be used to produce a mean effective at-satellite temperature for each sample area. (B) The resampled 2000 NDVI layer.

CHAPTER IV

RESIDENTIAL-STRUCTURE AND TEMPERATURE ANALYSIS

4.1. Qualitative analysis of the vegetation and temperature relationship

A qualitative analysis of the relationships between general larger spatial-scale vegetation distribution and surface temperature in residential areas reveals a noticeable negative correlation. Vegetation cover, which includes trees, grass, low-lying plants, and crops, influences the thermal properties of the terrestrial surface. In general, areas exhibiting vegetation cover that is relatively denser or thick correspond to areas with lower surface temperatures (e.g., forests). Compared to grassland areas or residential lawns, tree canopy can be considered as thick vegetation cover.

The Houston Metropolitan Area has an excellent model that highlights the correlation between vegetation cover abundance or type and temperature. Figure 4.1 illustrates the contrast in surface temperature for two residential developments. The general spatial distribution of temperature variation for these residential areas can be gleaned from the thermal image. Though qualitative analysis, the main difference observed between these two residential areas is the abundance of tree canopy. Figure 4.1A represents The Woodlands, a residential development that endeavors to preserve the older tree canopy while constructing new homes. Figure 4.1B represents Lake Houston, a neighborhood that cleared the land of vegetation prior to residential development. After clearing the older tree canopy, development takes place, lawns are plotted, and small trees are planted that evidentially grow to provide a cooling effect.

The thermal band from the 2000 Landsat ETM+ imagery is partially transparent and overlays the panchromatic band from the same data set. Figure 4.1 illustrates the differences in temperature between residential areas with significant tree canopy and residential areas lacking tree canopy; thereby, illustrating the contrast between the two development styles. The red areas represent higher emissivity values or temperatures that seem to radiate out from neighborhoods lacking tree canopy (Aniello et al., 1995), and the green areas represent cooler temperatures. The Woodlands, as a whole, appears much cooler than the Lake Houston neighborhood, even though the home density patterns and price values are approximately the same for both residential developments.
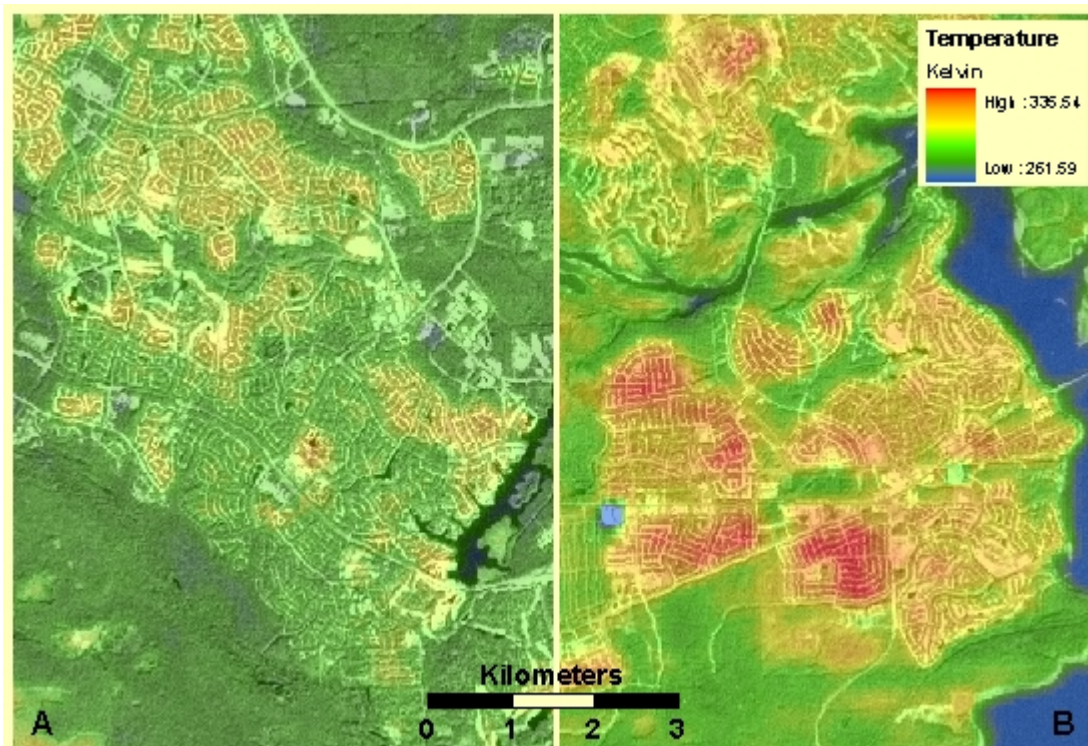
Figure 4.1. Temperature of residential areas with varying levels of tree canopy. The thermal band is placed over the panchromatic band from the 2000 Landsat ETM+ data. (A) The Woodlands, a residential neighborhood with significant tree canopy. (B) Lake Houston, a residential neighborhood lacking tree canopy. The Woodlands appears much cooler than the Lake Houston neighborhood.

Figure 4.2 displays the NDVI results from the 2000 Landsat ETM+ data and represents the same areas that are depicted in Figure 4.1. The red in Figure 4.2 represents a lack of vegetation, which corresponds to residential areas lacking tree canopy, and some transportation networks and urban development; the dark green and green regions represent areas with higher NDVI values and an abundance of green vegetation corresponding to forested areas and residential areas with significant tree canopy; the yellow areas represent an intermediate level of vegetation, and residential areas lacking tree canopy are located in these regions; and the blue represents water and an absence of vegetation. Considering the residential developments displayed in Figure 4.2, there appears to be a much larger area exhibiting low NDVI values in the Lake Houston neighborhood than in The Woodlands. The contrast between these two development styles highlights the importance of trees. The close association between the NDVI value and temperature is evident by visually comparing Figures 4.1 and 4.2. However, while it is clear that areas with high NDVI values have lower temperatures, the NDVI value alone does not provide information about the independent contributions of tree canopy and that of low-level vegetation cover toward lowering temperature. The micro-urban heat islands (Figure 4.1) seem to radiate out from individual center points of neighborhoods lacking tree canopy (Aniello et al., 1995).
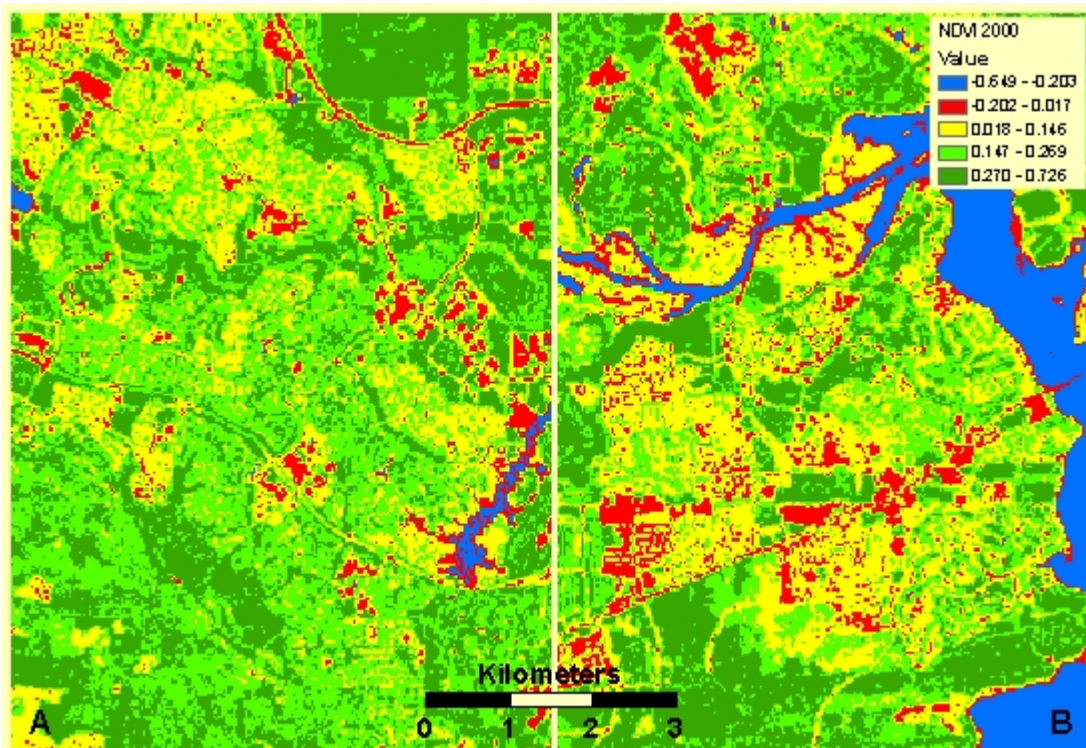
Figure 4.2. NDVI results of residential areas with varying levels of tree canopy. The image is derived from 2000 Landsat ETM+ data and corresponds to the areas depicted in Figure 4.1. (A) The Woodlands, a residential neighborhood with significant tree canopy. (B) Lake Houston, a residential neighborhood lacking tree canopy.

4.2. NDVI as an explanatory variable for surface temperature

The overall negative correlation between NDVI and surface temperature has been revealed in previous studies (Lo & Quattrochi, 2003; Lo et al., 1997; Gallo & Tarpley, 1996; Gallo et al., 1993). The mean NDVI values from the 2000 Landsat ETM+ data for each of the 442 stratified random residential sample areas plotted against the at-satellite temperatures for the same year show a strong negative correlation (Figure 4.3). When considering the R^2 value of 0.7675, the simple linear regression shows that about 77% of the variation observed for temperature can be explained by the NDVI, which is a measure of the overall abundance and/or quality of vegetation (Lillesand et al., 2004).
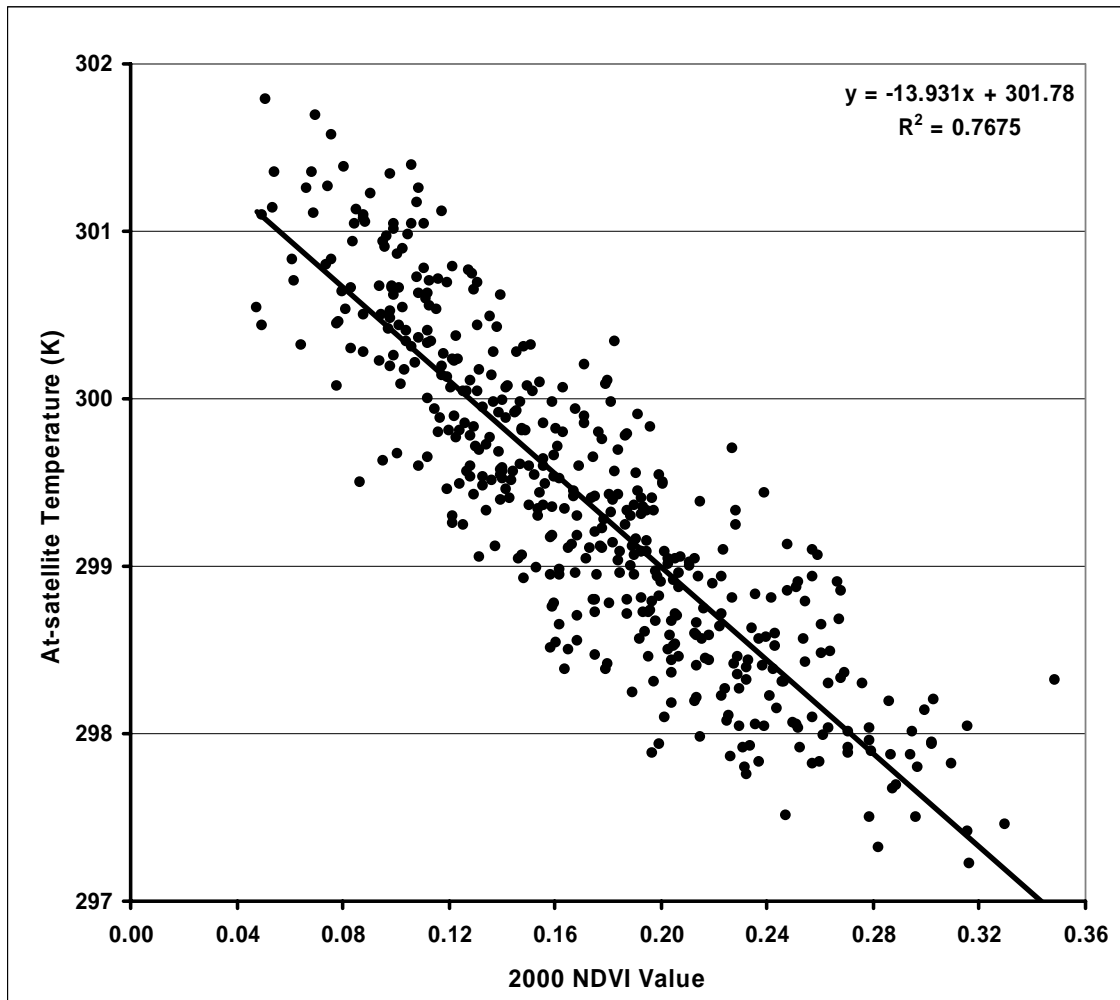
Figure 4.3. Correlation between temperature and the NDVI. A scatterplot of at-satellite temperature and 2000 Landsat ETM+ NDVI values. Approximately 77% of the variation in temperature can be explained by the NDVI value. The Pearson's correlation coefficient is -0.8761.

The NDVI alone, however, does not explain the degree to which variations in temperature are caused by the amount of different types of vegetation present in the residential environment. For concerned neighborhood planners, this information may be enormously helpful in mitigating the negative effects of micro-scale urban heat islands. In this study, an analysis of the correlations between NDVI, micro-scale vegetation measurements, and temperature for proximal residential sample areas shows that NDVI

may not be the best instrument for explaining the effects that different vegetation types have on surface temperature at the residential neighborhood scale. Residential areas can display similar relatively high NDVI values while exhibiting very different residential-structures. Green lawns can produce relatively high NDVI values, but they do not provide the same level of cooling as tree canopy. This may account for the seeming disagreement between the amount of total vegetation cover and temperature in some proximal residential areas. Therefore it is necessary to define the levels of cooling that both trees and low-level vegetation contribute independently.

In the following sections, residential areas exhibiting similar Total Vegetation Cover measurements but a wide range of vegetation types and combinations are analyzed. A measurement of the Total Vegetation Cover as a percentage of residential area based on the NDVI alone shows a relatively weak correlation to surface temperature (Figure 4.4). By incorporating feature height information, micro-scale vegetation measurements defining the abundance of various types and combinations of vegetation cover shows a much stronger correlation and can quantify the independent influence that different residential-structures have on surface temperature. The micro-scale vegetation measurements are evaluated as predictors of surface temperature. It is clear that a high NDVI value is desirable; however, the residential-structure that is needed to obtain the desired NDVI and a desired cooling effect in an individual neighborhood cannot be ascertained. The independent contributions of tree canopy and that of low-level vegetation cover toward lowering temperature must be quantified in order to help instruct planning and policy measures.
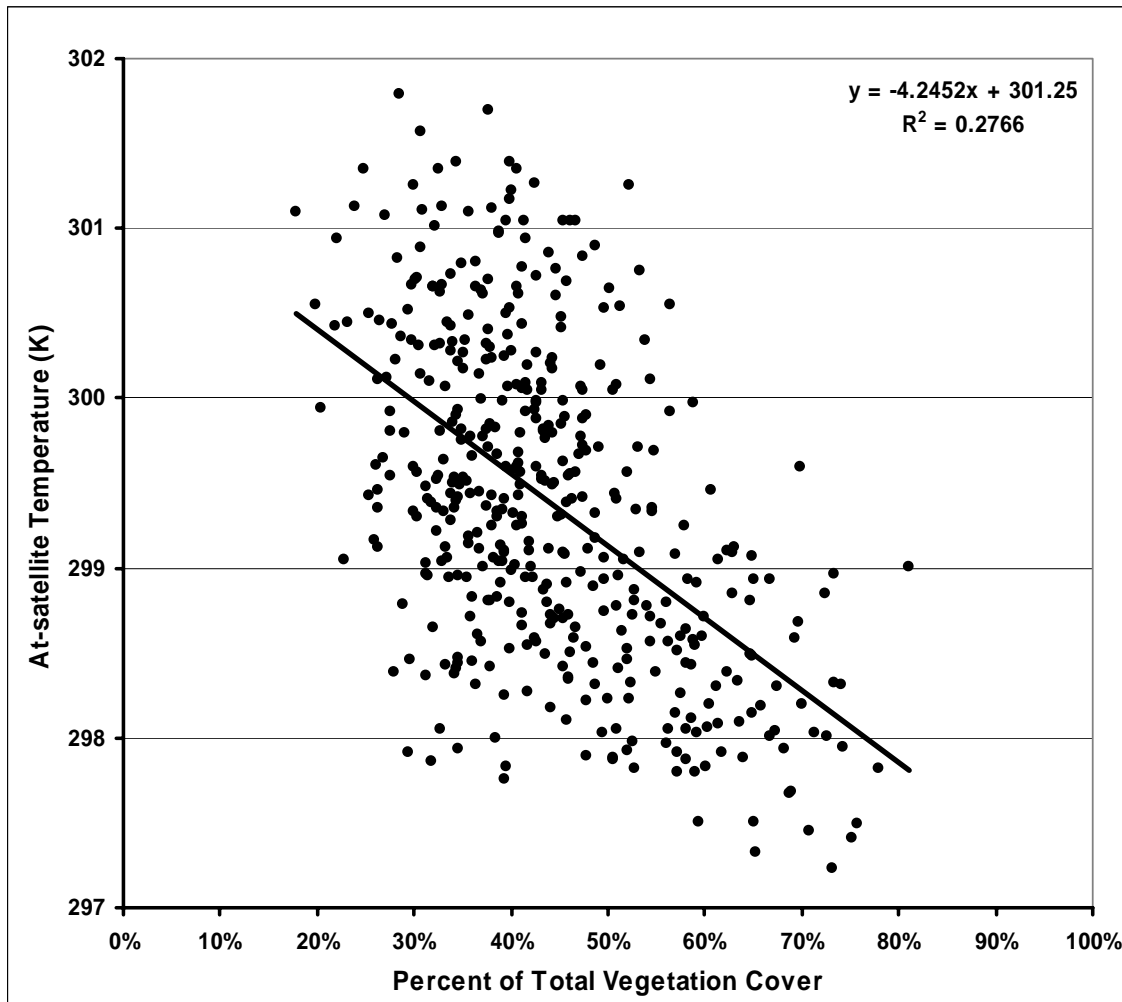
Figure 4.4. Correlation between temperature and Total Vegetation Cover. Only approximately 27% of the variation in temperature can be explained by Total Vegetation Cover. The Pearson's correlation coefficient is -0.5259.

4.3. Selection and sampling model for two representative regions

Given the examples of The Woodlands and Lake Houston neighborhoods described above, it is evident that by selecting a certain residential development style, a developer or city planner can greatly influence the thermal properties of the new neighborhood. However, the developer must know the specific residential-structure that should be employed to achieve a desired thermal goal, in terms of the amount of tree

canopy to retain versus the amount of grassy lawns to plot. Specifically selected to act as examples of two different types of neighborhoods in regard to residential-structure, the similarly sized neighborhood regions delineated in Figure 4.5 are analyzed in more detail. Region A represents a residential area lacking tree canopy. Region B represents a residential area with significant tree canopy. By comparing these two much smaller representative residential areas in close proximity to each other (unlike The Woodlands and the Lake Houston neighborhood), the geographically dependent variables relating to climate and elevation are essentially controlled. The distance from the center of Region A to the center of Region B is only 1,200 meters.
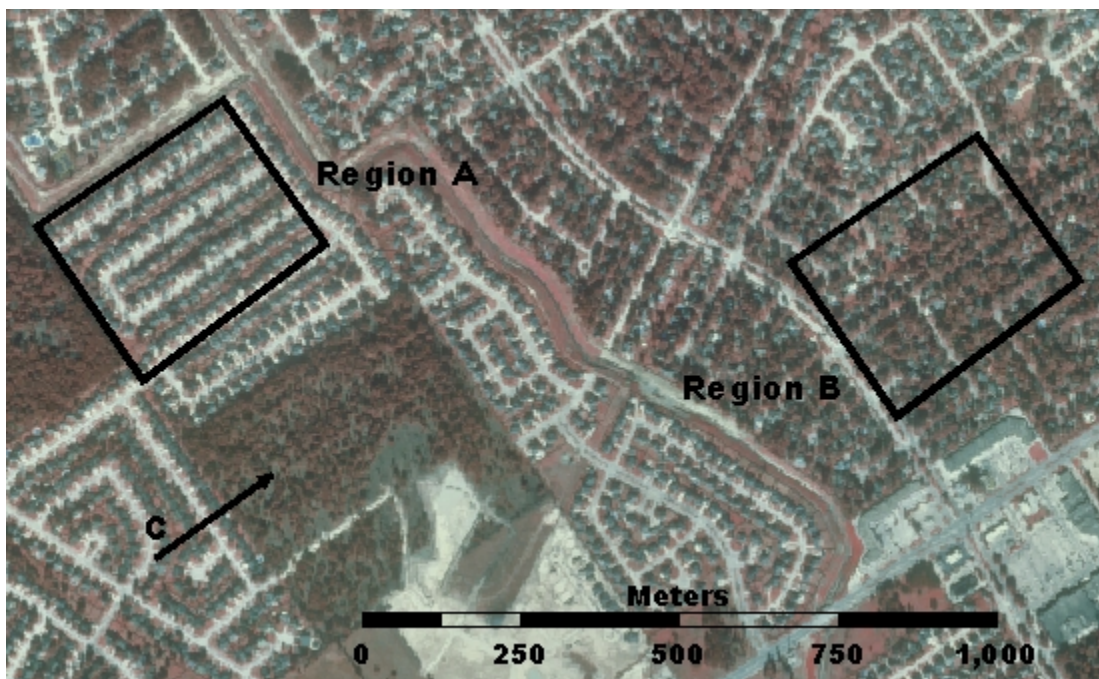
Figure 4.5. Two representative residential regions. A 1995 false color near-infrared composite DOQQ with 1 meter spatial resolution. Region A represents a residential area lacking tree canopy. Region B represents a residential area with significant tree canopy. The distance from the center of Region A to that of B is only 1,200 meters. The arrow at C points to an area that was developed between 1995 and 2000.

As described in Chapter III, the feature height threshold and the NDVI value threshold are identified in these two regions to calculate various micro-scale vegetation measurements. The residential-structure of each region displayed in Figure 4.5 is examined in relation to total area and in relation to each other. By acquiring NDVI values and feature heights from 1000 randomly selected points in each region, the general residential-structure pattern is revealed. Figure 4.6 is a scatterplot of the NDVI values and features heights for the 1000 random points in Region A, the residential area lacking tree canopy. Figure 4.7 is a scatterplot of the NDVI and features heights for the 1000 random points Region B, the residential area with significant tree canopy.
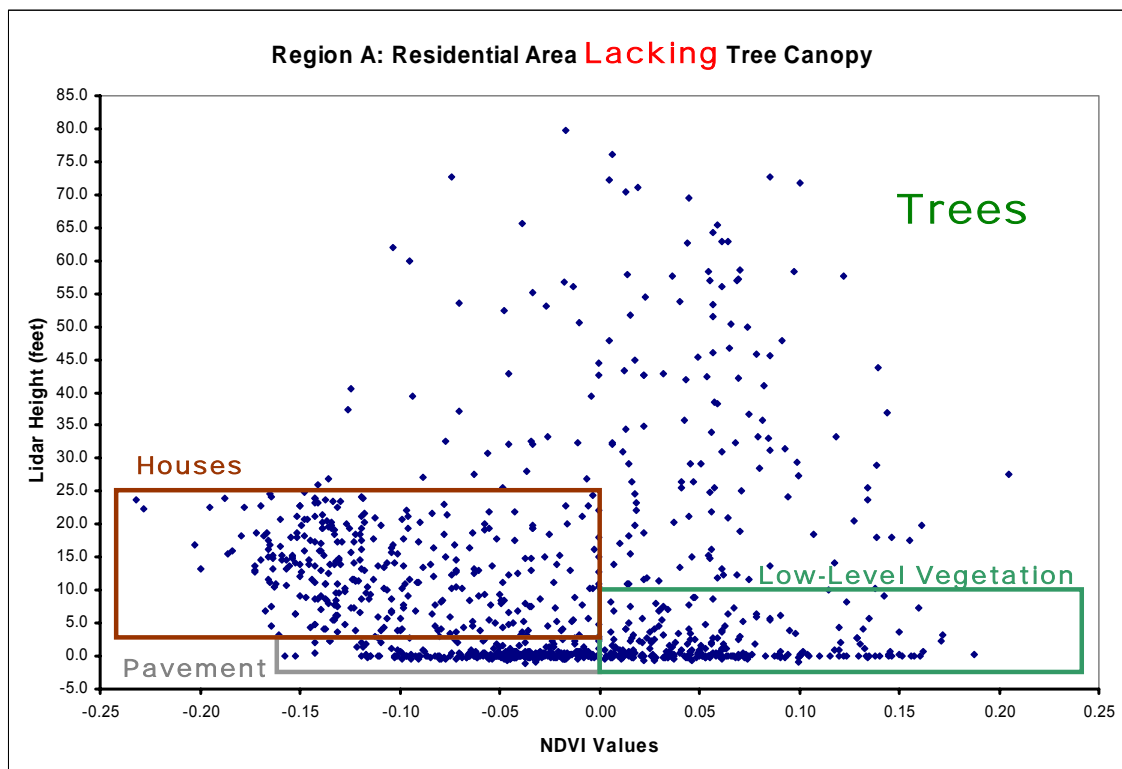
Figure 4.6. Scatterplot for Region A. The NDVI and features heights of 1000 random points in the residential area lacking tree canopy.
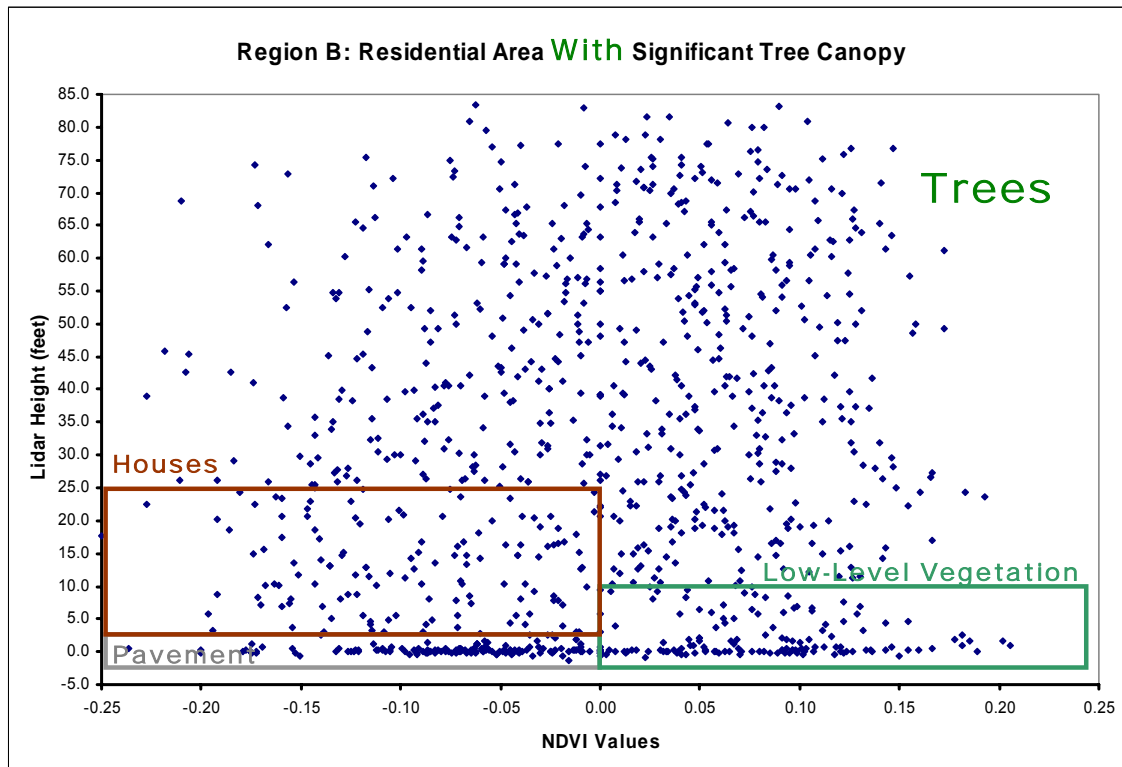
Figure 4.7. Scatterplot for Region B. The NDVI and features heights of 1000 random points in the residential area with significant tree canopy.

Using both Figures, a graphically aided assessment of the threshold values was conducted, and the scatterplots are labeled with the land-cover types assumed from the derived thresholds: trees, houses, pavement, and low-level vegetation. Although both scatterplots display a large number of points with NDVI values over the threshold of 0.00, most of those points for Region A are associated with low feature heights and represent grass and low-lying plants; most of the points for Region B with NDVI values > 0.00 have relatively high feature heights, which represent tree canopy. There are a relatively large number of points in Region B with low NDVI values and high feature heights. From examination, there are very few man-made features in these residential

regions that are taller than 25 feet; therefore, most of these points represent tall tree canopy with low NDVI values, most likely due to the season in which the 1995 DOQQ was acquired. The 1995 DOQQ, which is used to derive the NDVI values, was acquired in January, when the leaves were off the trees.

4.4. Residential-structure and temperature in two representative regions

The NDVI value and feature height value collected at each of the 1000 random points for each region were analyzed to derive micro-scale vegetation measurements that represent the residential-structure of each region. The statistical analysis results for each representative residential region are provided in Table 4.1. Based on the thresholding values, Region A has a Total Vegetation Cover of 48.20%, which is relatively similar to the Total Vegetation Cover of Region B: 58.47%. However, only 10.97% of the area of Region A is made up of Tall Tree Canopy compared to 48.40% for Region B. Although both regions have similar Total Vegetation Cover, only 8.85% of the total area of Region A has tall tree canopy with a high NDVI compared to 32.24% for Region B.

After the NDVI masking process, which lowers the tree canopy threshold to ≥ 10 feet, results show that only 15.98% of the total area of Region A has High NDVI Tree Canopy compared to 41.47% for Region B. The Total Tree Canopy measure for Region A is 18.09% compared to 57.63% for Region B. However, Region A has a much larger percentage of Low-Level Vegetation (32.22%) relative to Region B (17.00%). Adding the Total Tree Canopy to the Low-Level Vegetation yields 50.31% for Region A and 74.63% for Region B.

Analysis shows that, in terms of area, both regions have similar amounts of Total Vegetation Cover (i.e., NDVI values > 0). In contrast to each other, however, the Total Tree Canopy measurement is much lower for Region A than Region B. Moreover, the vegetative cover for Region A is made up of mostly Low-Level Vegetation (grasses or low-lying plants) and Region B's is made up of mostly tree canopy. The percentage of Total Vegetation Cover for Region A that is tree canopy (LIDAR feature heights ≥ 10 feet) is only 33.15%. The percentage of the Total Vegetation Cover for Region B that is tree canopy is 70.93%.

Table 4.1
Residential-Structure Statistics of Representative Neighborhoods

	Region	A	B
	Total square meters	104,434	101,464
Land cover variable	Description	Percent total area	Percent total area
Total Vegetation Cover	NDVI value > 0	48.20	58.47
Tall Tree Canopy	LIDAR feature heights ≥ 25 (ft)	10.97	48.40
tall trees w/ high NDVI	LIDAR ≥25 and NDVI > 0	8.85	32.24
tall trees w/ low NDVI	LIDAR ≥25 and NDVI ≤ 0	2.11	16.16
High NDVI Tree Canopy	LIDAR ≥10 and NDVI > 0	15.98	41.47
Total Tree Canopy	LIDAR ≥10 and NDVI > 0 or LIDAR ≥ 25	18.09	57.63
Low-Level Vegetation	NDVI value > 0 and LIDAR < 10	32.22	17.00
Total Tree Canopy and Low-Level Vegetation together		50.31	74.63
Mean 1995 NDVI value	DOQQ January 23, 1995	-0.0041	-0.0269
Mean 2000 NDVI value	Landsat ETM+ January 10, 2000	0.1132	0.2549
Mean at-satellite temperature (K)		300.985	298.033

After establishing the differences and similarities between the two representative regions regarding amount of Total Vegetation Cover and Total Tree Canopy, the regions are examined in regard to their mean effective at-satellite temperatures. The short

distance between the regions reduces the influence of any climate variability. However, their mean effective at-satellite temperatures are much different as illustrated by Figure 4.8, which is the 2000 Landsat ETM+ thermal band laid over a 2002 natural color DOQQ. The mean effective at-satellite surface temperature for Region A, which represents a residential neighborhood lacking tree canopy, is 300.985 Kelvin. The mean effective at-satellite surface temperature for Region B, which represents a residential neighborhood with significant tree canopy, is 298.033 Kelvin (Table 4.1). This is a difference of 2.982 Kelvin, or almost 3º Celsius. Even though the regions are proximal and they exhibit similar Total Vegetation Coverage, the thermal properties are quite different. The determining factor seems not to be the coverage, but the abundance or dearth of certain types of vegetation coverage.

The neighborhood, marked as "C" and pointed out in Figures 4.8 and 4.5, is a newer residential development built between 1995 and 2000. This new development was built after the tree canopy, present in 1995 (Figure 4.5), was removed. The micro-urban heat island effect is observable; the highest temperature (302.203 Kelvin) is near the center of the neighborhood and the temperatures decrease with distance from the center. By removing the tree canopy, a new micro-urban heat island was created between 1995 and 2000. The highest temperature observed in Region A is also 302.203 Kelvin. The Low-Level Vegetation present in Region A provides less of a cooling effect compared to tree canopy. If a certain amount of tree canopy was retained during development, the impact of the heating effect would have been decreased. So, how much of the tree canopy should have been retained?
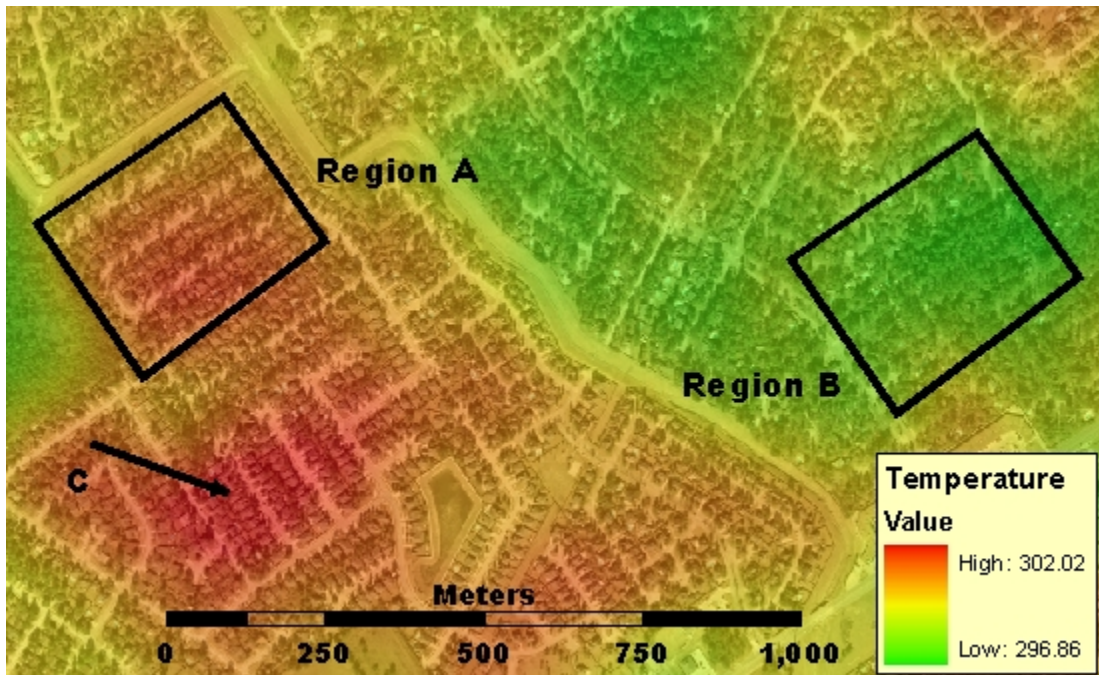
Figure 4.8. Thermal characteristics of two representative residential regions. A smoothed partially transparent 2000 Landsat ETM+ thermal band over a 2002 DOQQ (1-foot spatial resolution). The distance from the center of Region A to that of B is only 1,200 meters. The mean effective at-satellite temperature is 300.985 Kelvin for Region A and 298.033 Kelvin for Region B. This is a difference of 2.982 Kelvin, or almost 3º Celsius. The arrow at C points to an area that was developed between 1995 and 2000.

Research has shown that vegetation indices and surface temperature have an overall strong negative correlation (Weng et al., 2004; Kustas et al., 2003; Lo & Quattrochi, 2003; Lo et al., 1997; Gallo & Tarpley, 1996; Gallo et al., 1993; Roth et al., 1989). Therefore, it is well established that having an overall high NDVI value in a neighborhood will mitigate the heating effect. However, the specific type of residential-structure needed to obtain an overall high NDVI value is less well established. Moreover, the NDVI value does not explain the degree to which certain types and amounts of residential vegetation cool a neighborhood. By analyzing the results from the two representative regions, it appears that the micro-scale vegetation measurements

could provide more illuminating variables, regarding the effects of residential-structure on temperature. This high spatial resolution analysis using LIDAR data and the false color near-infrared DOQQ has provided detailed information regarding the type and abundance of certain vegetation at a neighborhood scale for the two chosen representative regions. A more robust variation of this micro-scale vegetation measurement approach, focused on residential-structure, is used to analysis 442 sample areas and is aimed at quantifying the level of influence that various types and amounts of residential land-cover have on temperature at a neighborhood scale.

4.5. Residential-structure as a more explanatory variable

By incorporating a high-resolution NDVI image, LIDAR data, and a residential sampling technique, the micro-scale vegetation measurement approach provides information about residential-structure. Using the binary grids described in Chapter III, descriptive statistics for each of the 442 stratified random residential sample areas are derived. These descriptive statistics correspond to the percentage of the total area that a particular variable populates within each residential sample area. The statistical values were extracted from the grid cells in each sample area by means of a relatively simple programming function written in C++ program language. Each grid statistic corresponding to a specific micro-scale vegetation measure is analyzed as a predictor variable, where temperature is the response variable. In other words, the variables that characterize residential-structure act as independent or explanatory variables for predicting the mean effective at-satellite temperature (the dependent variable) that may

be observed for residential neighborhoods. In addition, the mean 2000 NDVI value and the mean feature height in each sample area are evaluated against temperature.

Utilizing the statistical values of the 442 residential sample areas, a simple linear regression model is used to identify correlations. The levels of influence that various types and amounts of vegetation have on temperature have been separately analyzed, by evaluating the micro-scale vegetation measurements in terms of their relationship to effective at-satellite surface temperature with the simple linear regression model. Table 4.2 provides a summary of the results and a description of each measurement that represent residential-structure. As noted earlier, Total Vegetation Cover based on the NDVI alone shows a relatively weak correlation to effective at-satellite surface temperature. However, the Total Tree Canopy measurement shows a very strong correlation to temperature. Although the mean 2000 NDVI value also shows a strong correlation to temperature, it does not describe the residential-structure of the neighborhood in which the NDVI value was recorded by the Landsat ETM+ sensor.

Table 4.2

Residential-Structure Statistics Plotted against Temperature

Land cover variable	Description	R^2	Pearson's r
Total Vegetation Cover	NDVI value > 0	0.2766	-0.5259
Above Ground Features	LIDAR ≥10	0.6283	-0.7927
High NDVI Tree Canopy	LIDAR ≥10 and NDVI > 0	0.6249	-0.7905
Tall Tree Canopy	LIDAR feature heights ≥ 25 (ft)	0.7841	-0.8855
Total Tree Canopy	LIDAR ≥10 and NDVI > 0 or LIDAR ≥ 25	0.7879	-0.8876
Mean Feature Height	Mean LIDAR feature height value	0.7465	-0.8640
Mean 2000 NDVI value	Landsat ETM+ January 10, 2000	0.7675	-0.8761

From the linear regressions, scatterplots have been created that plot the effective at-satellite surface temperature against the following explanatory variables:

1) The Total Vegetation Cover (Figure 4.9);

2) The Above Ground Features (Figure 4.10);

3) High NDVI Tree Canopy (Figure 4.11);

4) Tall Tree Canopy (Figure 4.12);

5) Total Tree Canopy (Figure 4.13).

6) The mean feature height (Figure 4.14); and

7) The mean 2000 NDVI value (Figure 4.15).
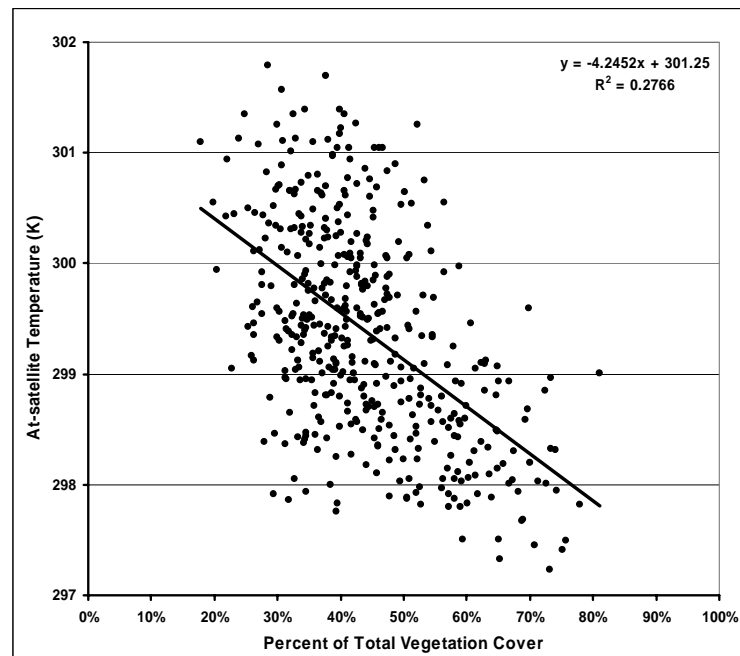
Figure 4.9. Scatterplot of temperature and Total Vegetation Cover. Only about 28% of the variation in temperature can be explained by this measurement. The Pearson's correlation coefficient is -0.5259.
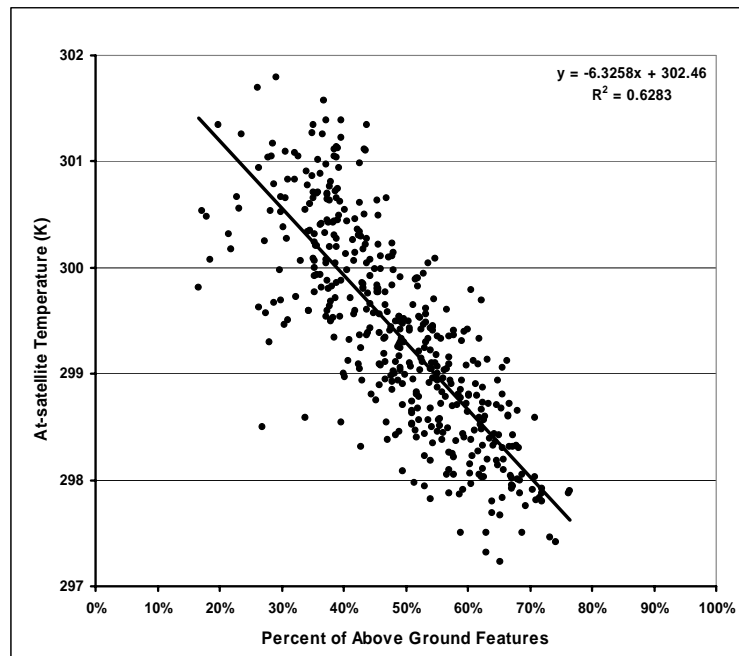
Figure 4.10. Scatterplot of temperature and Above Ground Features. Approximately 63% of the variation in temperature can be explained by this measurement. The Pearson's correlation coefficient is -0.7927.
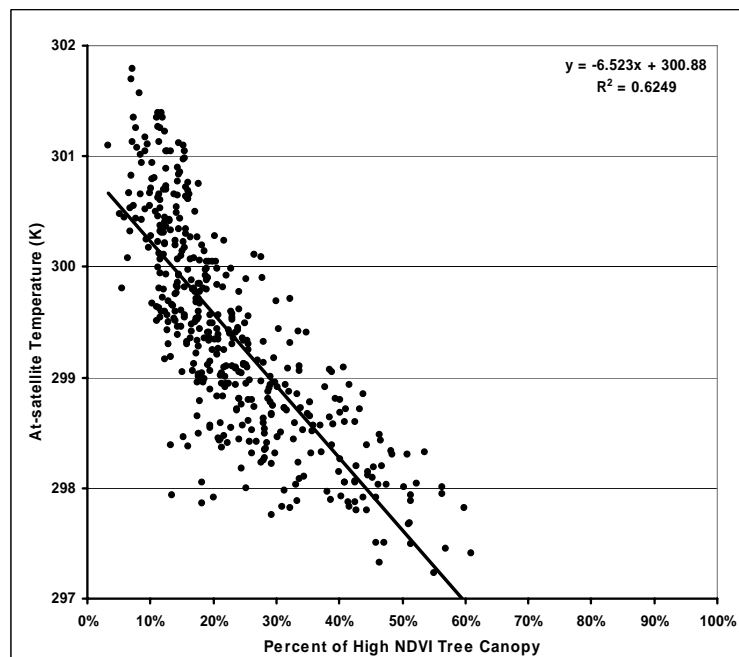
Figure 4.11. Scatterplot of temperature and High NDVI Tree Canopy. Approximately 62% of the variation in temperature can be explained by this measurement. The Pearson's correlation coefficient is -0.7905.
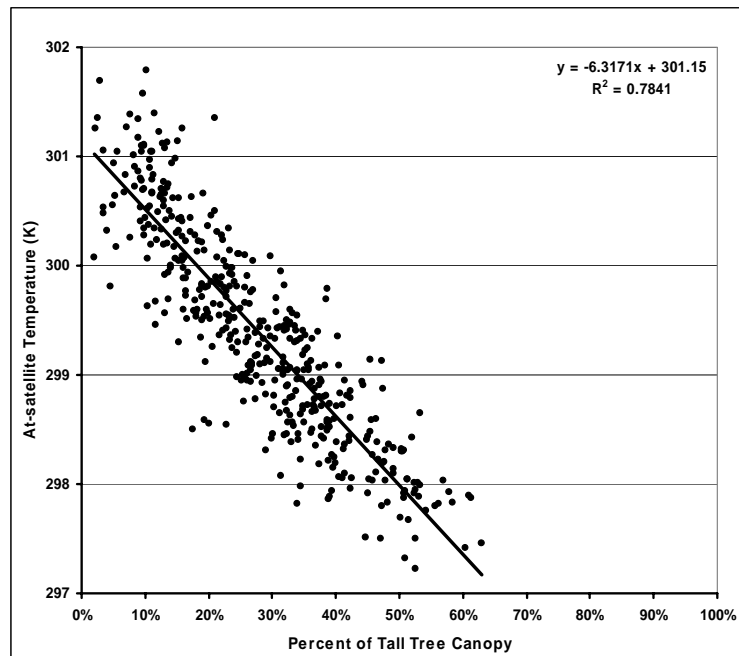
Figure 4.12. Scatterplot of temperature and Tall Tree Canopy. Approximately 78% of the variation in temperature can be explained by this measurement. The Pearson's correlation coefficient is -0.8855.
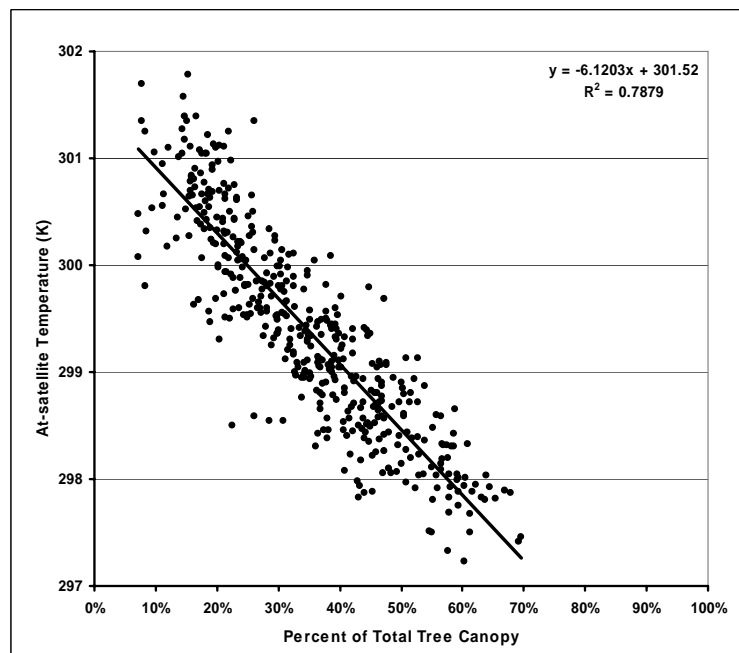
Figure 4.13. Scatterplot of temperature and Total Tree Canopy. Approximately 79% of the variation in temperature can be explained by this measurement. The Pearson's correlation coefficient is -0.8876.
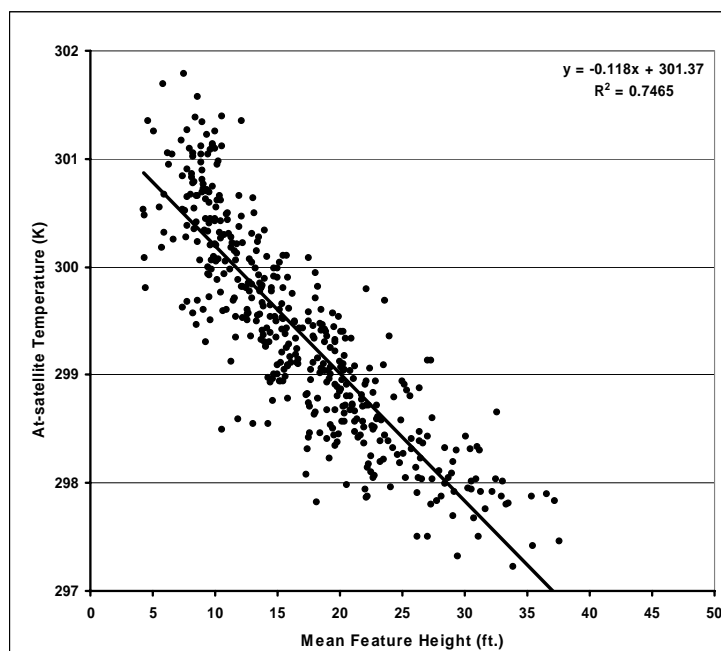
Figure 4.14. Scatterplot of temperature and mean feature height. Approximately 75% of the variation in temperature can be explained by this measurement. The Pearson's correlation coefficient is -0.8640.
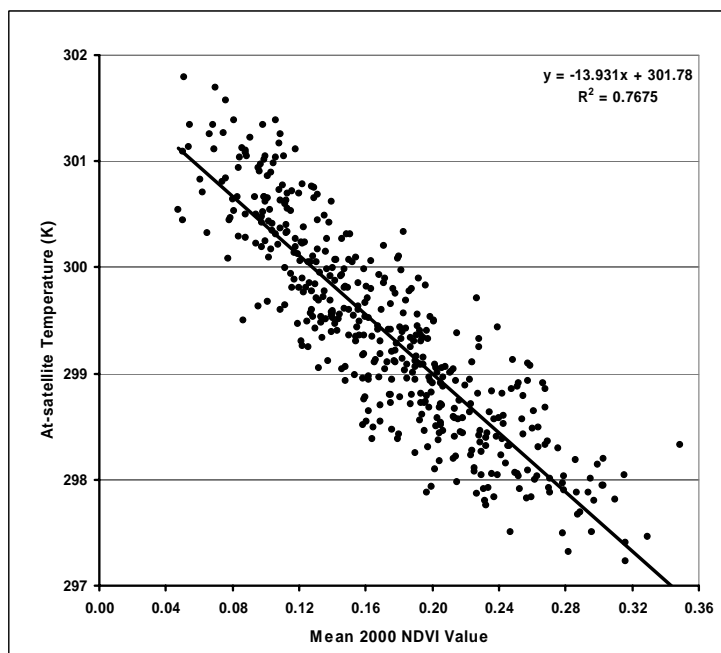
Figure 4.15. Scatterplot of temperature and mean 2000 NDVI value. Approximately 77% of the variation in temperature can be explained by NDVI. The Pearson's correlation coefficient is -0.8761.

The simple linear regression shows that the Total Tree Canopy measurement can explain about 79% of the variation observed in temperature, considering the coefficient of determination (R^2 value) of 0.7879. The regression equation that quantifies the influence of this micro-scale vegetation measure on temperature change is as follows:

$$T_K = 301.52 - 0.061203 X_{TTC} \tag{4.1}$$

where X_{TTC} is the percent of area covered by Total Tree Canopy in a residential neighborhood, and T_K is the effective at-satellite surface temperature in Kelvin. Therefore, a 1% change in the area covered by Total Tree Canopy in a neighborhood changes Kelvin ±0.061203. Table 4.3 illustrated the expected temperatures in the residential study area given the percent of Total Tree Canopy (X_{TTC}), and the accumulation columns show the value of Total Tree Canopy as it relates to temperature. The Kelvin values have been converted to equivalent degrees Celsius and Fahrenheit. A 10% decrease in the area of Total Tree Canopy means an increase of 0.61° C or 1.10° F.

Table 4.3
Value of Total Tree Canopy

Percent of X_{TTC}	Change in °Celsius		Change in °Fahrenheit	
	Predicted °C	Δ° C	Predicted °F	Δ° F
100	22.25	0.00	72.05	0.00
90	22.86	0.61	73.15	1.10
80	23.47	1.22	74.25	2.20
70	24.09	1.84	75.35	3.30
60	24.70	2.45	76.46	4.41
50	25.31	3.06	77.56	5.51
40	25.92	3.67	78.66	6.61
30	26.53	4.28	79.76	7.71
20	27.15	4.90	80.86	8.81
10	27.76	5.51	81.96	9.91
0	28.37	6.12	83.07	11.02

In order to derive the *t*-value to test the significance of the correlation between the dependent variable (temperature) and the independent variable (Total Tree Canopy) using a two-tailed Student's t distribution test statistic, the estimated standard error (S_r) was obtained using the following equation:

$$S_r = \sqrt{\frac{1-r^2}{n-df}} = \sqrt{\frac{1-(0.7849)^2}{442-2}} = 0.0295729664 \qquad (4.2)$$

where *r* is the Pearson's r correlation coefficient, *n* is the number of residential sample areas, and *df* is the degrees of freedom. A hypothesis test was established, where the null hypothesis is $H_0 : \rho = 0$ and the alternative hypothesis is $H_A : \rho \neq 0$, and ρ is the p-value or probability that the Total Tree Canopy is not correlated to temperature. The following equation was used to obtain the *t*-value:

$$t = \frac{r}{S_r} = \frac{0.7849}{0.0295729664} = 26.54 \qquad (4.3)$$

The *t*-value is greater than $t(\alpha/2, n-df)$, which is 2.576 according the *t* distribution table, where α is 0.01. Therefore, the null hypothesis is rejected, and there is a 99% confidence level that the results express a statistically significant correlation between the temperature and Total Tree Canopy and are not randomly derived.

The Total Tree Canopy is not the only vegetation cover present in a neighborhood, and it is not the only vegetation that influences temperature. By removing the High NDVI Tree Canopy from the Total Vegetation Cover measurement, a Low-Level Vegetation grid is defined. Areas of Low-Level Vegetation have a relatively high

NDVI value (> 0.0) and a low LIDAR feature height (< 10 feet). These areas consist of residential lawns, low-lying plants, and even some very small trees.

If a developer clears an area of vegetation prior to construction, Low-Level Vegetation would typically be the only vegetation present soon after construction is completed. Usually, residential lawns are plotted and small trees are planted in the new residential development by the new residents. Figure 4.16 provides an example of a newly constructed neighborhood; the micro-scale vegetation measurement grids overlay the 1995 false color near-infrared composite DOQQ. Sample area #5 of the 442 stratified random residential sample areas highlights the residential-structure of a typical newly developed residential neighborhood. Total Tree Canopy is 9.79% of sample area #5 (Figure 4.16A); Low-Level Vegetation covers 36.19% (Figure 4.16B); and the mean effective at-satellite surface temperature for sample #5 is 301.049 Kelvin. If the vegetation in a residential-structure similar to sample area #5 provides a cooling effect, it would have to come from the Low-Level Vegetation, primarily. However, there is some tree canopy present; therefore, the micro-scale vegetation measurements must be analyzed together.

Figure 4.16. A typical newly developed residential neighborhood. Vegetation measurement grids overlay the 1995 false color near-infrared composite DOQQ. The mean at-satellite surface temperature for sample area #5 is 301.049 Kelvin. (A) The green areas represent Total Tree Canopy: 9.79% for sample area #5. (B) The light green areas represent Low-Level Vegetation: 36.19% for sample area #5.

The simple linear regression model cannot be used to quantitatively evaluate the influence that Low-Level Vegetation alone has on temperature variation, because the tree canopy is removed from the Low-Level Vegetation grid. In actual fact, the Total Tree Canopy grid has been removed of Low-Level Vegetation; therefore, the simple linear regression results for Total Tree Canopy can only represent a partial assessment. The strong correlation results, however, indicate that Low-Level Vegetation certainly has a smaller impact on temperature variation in residential areas.

In order to account for the variation in temperature (a single response variable), when several explanatory variables exist, a multiple regression analysis is employed (Burt & Barber, 1996). This approach yields a single explanatory equation that

quantifies the independent influence that Total Tree Canopy and Low-Level Vegetation separately have on temperature variations observed in the residential study area (Burt & Barber, 1996). The mean at-satellite temperature for each sample area represents the dependent variable, and the Total Tree Canopy and Low-Level Vegetation measures are the independent variables. These independent variables also represent the residential-structure in terms of vegetation type and amount. The multivariate least squares regression equation that quantifies the contribution that each of these micro-scale vegetation measures has on temperature is as follows:

$$T_K = 302.277 - 0.06872 X_{TTC} - 0.02344 X_{LLV} \qquad (4.4)$$

where X_{TTC} is the percent of area covered by Total Tree Canopy in a residential neighborhood, X_{LLV} is the percent of area covered by Low-Level Vegetation in a residential neighborhood, and T_K is the effective at-satellite surface temperature in Kelvin. The coefficient of determination or R^2 value for the equation is 0.813 and the Pearson's correlation coefficient is -0.902; therefore, the Total Tree Canopy and the Low-Level Vegetation combined can explain about 81% of the variation observed in temperature for the residential study area. This is a small but significant improvement on the simple linear regression for Total Tree Canopy of about 79% and the mean 2000 NDVI value of about 77%.

More importantly, however, the multivariate equation provides a quantitative value for the level of influence that each of the micro-scale vegetation measures separately has on temperature. For neighborhood planners that are concerned with mitigating the micro-scale urban heat island effect in a residential area, this information

is extremely helpful. A residential-structure can be planned that will allow for lawns and new small trees, but will also retain a certain amount of the older tree canopy during construction. Given the explanatory equation, increasing or decreasing the Total Tree Canopy by 1% would yield an expected change in temperature of ±0.06872 Kelvin, and by in increasing or decreasing the Low-Level Vegetation by 1%, a change of ±0.02344 Kelvin can be expected. Table 4.4 lists a number of the sample areas representing various residential-structures listed according to predicted temperature change, given the explanatory equation and the micro-scale vegetation measures. The first row of values represents an area that is forested and undeveloped. The first sample area (Figure 4.17) showed the lowest predicted temperature (297.171 Kelvin); the following rows or samples are ranked according to predicted temperature; the last sample (Figure 4.18) is ranked 442 and showed the highest predicted temperature (301.112 Kelvin).

Table 4.4
Examples of Temperature Change for Various Residential-Structures

Rank	Percent of X_{TTC}	Percent of X_{LLV}	Predicted Kelvin	Change in °Celsius		Change in °Fahrenheit	
				°C	Δ° C	°F	Δ° F
	90.0	10.0	295.858	22.71	0.00	72.87	0.00
1	69.6	13.9	297.171	24.02	1.31	75.24	2.36
40	56.5	13.4	298.080	24.93	2.22	76.87	4.00
80	49.7	12.7	298.565	25.41	2.71	77.75	4.87
120	40.8	27.8	298.825	25.67	2.97	78.21	5.34
140	42.2	13.1	299.073	25.92	3.21	78.66	5.79
180	37.3	17.1	299.315	26.16	3.46	79.10	6.22
220	34.7	16.0	299.516	26.37	3.66	79.46	6.58
260	30.0	18.2	299.793	26.64	3.94	79.96	7.08
300	22.0	30.8	300.045	26.89	4.19	80.41	7.54
340	17.0	36.9	300.244	27.09	4.39	80.77	7.89
380	18.6	27.8	300.350	27.20	4.49	80.96	8.09
420	15.6	23.6	300.655	27.50	4.80	81.51	8.63
442	12.0	14.5	301.112	27.96	5.25	82.33	9.46

Figure 4.17. Sample with the lowest predicted temperature. Sample #69 has a Total Tree Canopy measure of 69.55% and a Low-Level Vegetation measure of 13.91%. Of the 442 samples it had the lowest predicted temperature at 297.171 Kelvin and an observed temperature of 297.456 Kelvin. (A) 2002 DOQQ (1-foot resolution). (B) Micro-scale vegetation measurements overlying the 1995 DOQQ (1m resolution).

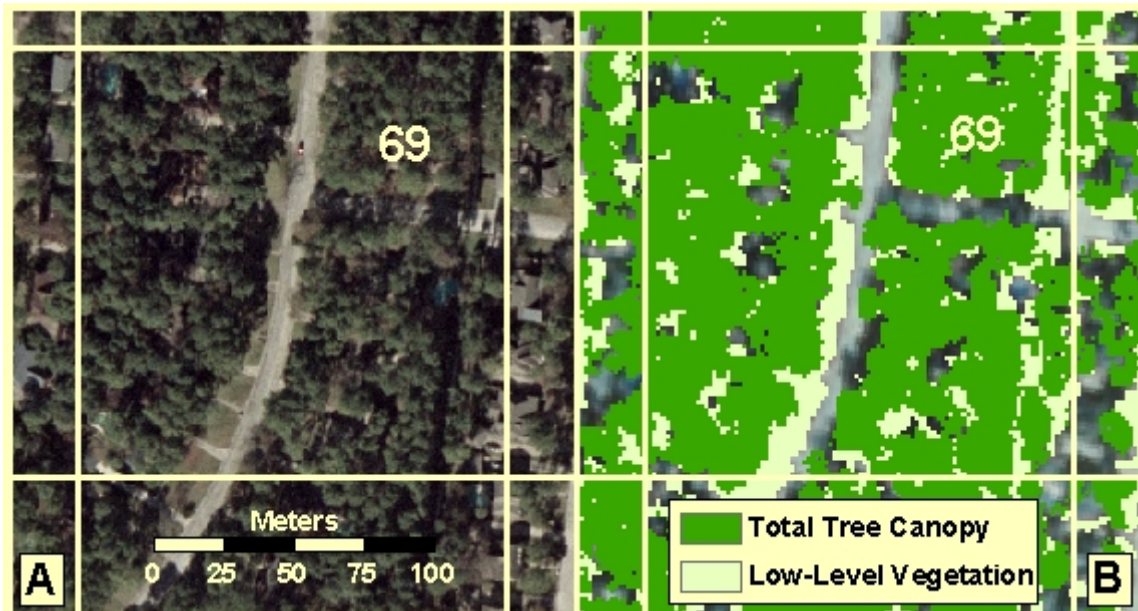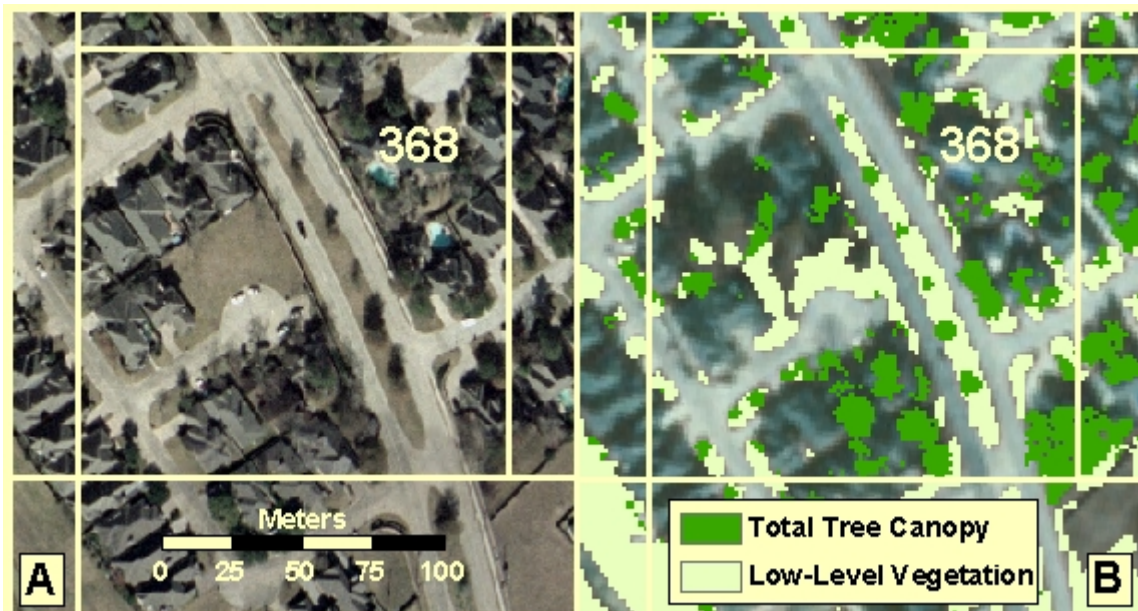Figure 4.18. Sample with the highest predicted temperature. Sample #368 has a Total Tree Canopy measure 12.03% and a Low-Level Vegetation measure of 14.45%. Of the 442 samples it had the highest predicted temperature at 301.112 Kelvin and an observed temperature of 301.094 Kelvin. (A) 2002 DOQQ (1-foot resolution). (B) Micro-scale vegetation measurements overlying the 1995 DOQQ (1m resolution).

A summary of the multiple regression analysis results is provided in Table 4.5. The standard deviation error (Std. Error) for the coefficients is utilized to obtain the 95% lower and upper bound confidence intervals. Given the t-values, the test of significance (Sig. Test) values are well beyond the requirements needed for 95% confidence. With a VIF of 1.477, collinearity the between variables is not an issue. In regard to the residuals, the explanatory equation overestimated the temperature for sample area #91 at 299.633 K; the actual observed temperature is 298.496 K; this represents the minimum residual: -1.13675. Figure 4.19 illustrates the problem. Sample area #91 is in close proximity to a forested area that has much lower temperature, which strongly influences the temperature in the sample area. The maximum residual represents an underestimate of temperature for sample area #195. The explanatory equation predicted the temperature at 300.157 K; the actual observed temperature is 1.18978 K higher or 301.347 K. Figure 4.20 illustrates the problem in sample #195. There are a number of unusually tall houses in the sample area that are higher than the tall tree canopy threshold value of 25 ft. These houses were measured as Total Tree Canopy. The average standard deviation from the temperature is 0.41457 K for the equation.

Table 4.5
Multiple Regression Analysis Results

Pearson's correlation coefficient		r = -0.902		Coefficient of determination		R^2 = 0.813
	Coefficients				95% Confidence Interval	
Variables	Equation	Std. Error	t-values	Sig. Test	Lower Bound	Upper Bound
Constant	302.277	0.11200	2692.850	0.00	302.056	302.498
X_{TTC}	-0.06872	0.00173	-39.722	0.00	-0.07212	-0.06532
X_{LLV}	-0.02344	0.00306	-7.649	0.00	-0.02946	-0.01742
	Minimum	Maximum	Mean	Std. Dev.	Variance Inflation Factor (VIF)	
Residuals	-1.13675	1.18978	0.00	0.41457	1.477	
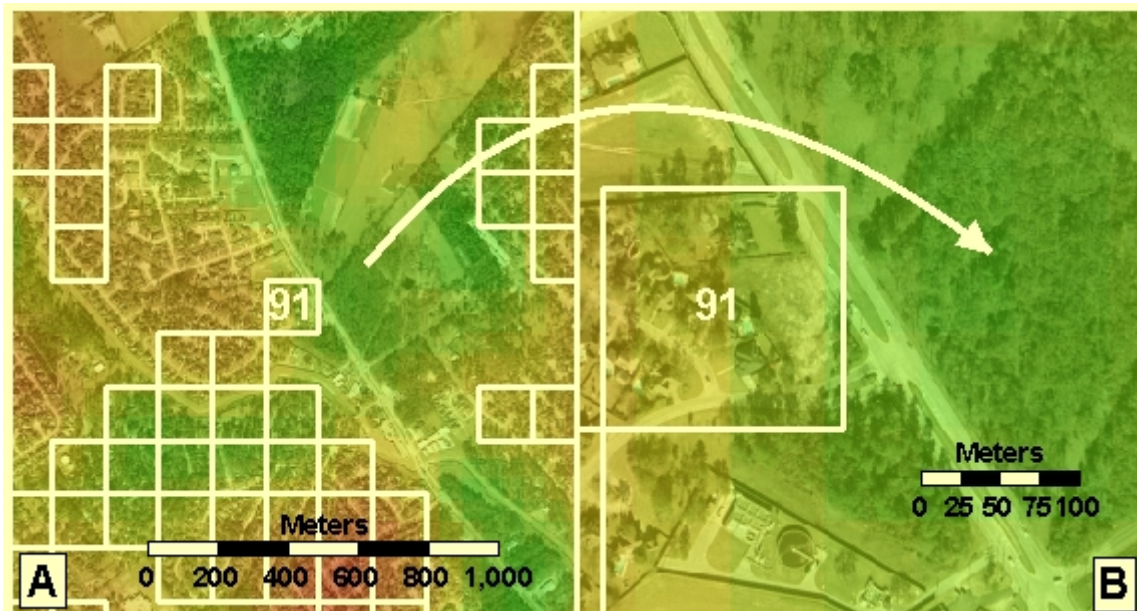
Figure 4.19. Overestimate of temperature. The observed temperature for sample area #91 is 298.496 K; the explanatory equation over predicted the temperature at 299.633 K. This represents the minimum residual value of -1.13675. (A) The sample area is proximal to a forested area that provides a cooling effect. (B) The east side of sample area #91 is noticeably cooler, due to the strong influence of the forest to the east.

Figure 4.20. Underestimate of temperature. The observed temperature for sample area #195 is 301.347 K; the explanatory equation under predicted the temperature at 300.157 K. This represents the maximum residual value of 1.18978. (A) There are a number of houses in the sample that are higher than the tall tree canopy threshold value of 25 ft. (B) These houses were measured as part of the Total Tree Canopy.

The micro-scale vegetation measurement approach, coupled with the multiple regression analysis has provided a means to quantify the residential-structure of a neighborhood and the influence that various residential designs have on temperature. The descriptive statistics in Table 4.6 provide general information about the larger sample area as a whole. Figure 4.17 and 4.18, as noted above, illustrate the extreme cases. Sample area #69 (Figure 4.17) represents a neighborhood with a relatively lower than average temperature (297.456 K), due to its residential-structure. It has approximately double the area of X_{TTC} (69.55%) than the overall average of the 442 residential sample areas, in addition to the 13.91% of X_{LLV}. Sample area #368 (Figure 4.18) represents a neighborhood with a relatively higher than average temperature (301.094 K). With an X_{TTC} of 12.03% and an X_{LLV} of 14.45%, both well below average, sample area #368 represents a neighborhood with an undesirable residential-structure.

Table 4.6
Descriptive Statistics for 442 Residential Sample Areas

Measure	Mean	Std. Dev.
Total Tree Canopy (X_{TTC})	34.94%	13.90%
Low-Level Vegetation (X_{LLV})	20.99%	7.85%
2000 NDVI Value	0.17220	0.06026
Observed Temperature (K)	299.384	0.95826
Predicted Temperature (K)	299.384	0.86394
Predicted Temperature (°C)	26.23	0.86394
Predicted Temperature (°F)	79.22	1.55508
Residuals	1.83E-05	0.41457

With a more precise understanding of the independent contributions of tree canopy and that of low-level vegetation cover toward lowering temperatures in a

residential neighborhood, developers and city planners can direct construction in a more exacting manner to mitigate the problems caused by micro-urban heat islands. The micro-urban heat islands, visible in Figure 4.21, radiate out from individual center points and influence the surrounding areas. On the other hand, the cooler areas with a more beneficial residential-structure also influence their surrounding. By constructing neighborhoods that retain a specific amount of older tree canopy in addition to plotting lawns and planting smaller trees, the newer development would not only have lower temperatures, it could help provide a relative overall cooling effect for a whole city.
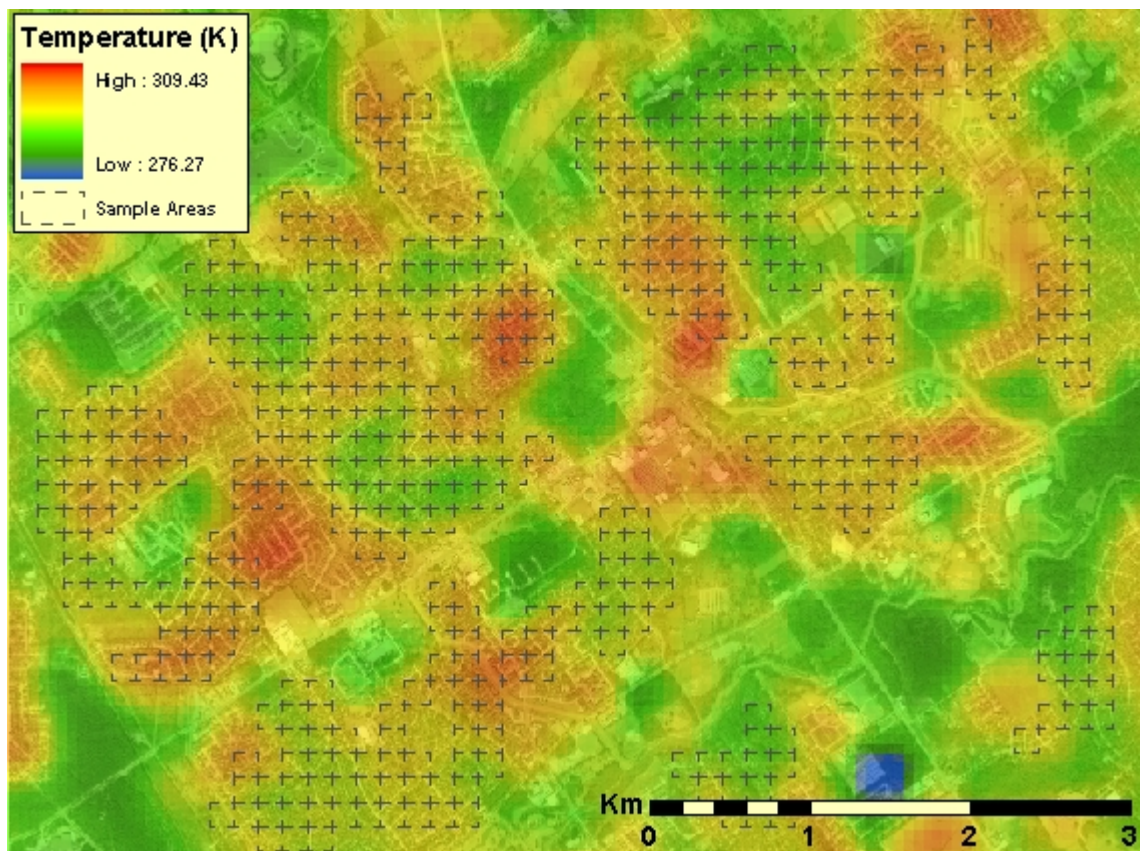
Figure 4.21. The residential micro-urban heat island effect. Higher temperatures radiate out from a number of individual center points and influence their surroundings. At the same time, cooler areas with a more beneficial residential-structure, in regards to temperature, also influence their surroundings.

CHAPTER V

CONCLUSIONS

The extent and magnitude of the larger urban heat island over the Houston Metropolitan Area has been well defined (Streutker, 2003; 2002). This large scale urban heating is an example of anthropogenic climate modification. Urban sprawl and deforestation are the main contributors. Houston is the only major city in the United States lacking comprehensive city zoning ordinances. That fact coupled with Houston's rapid economic growth has allowed market forces to drive commercial location decisions and not purposeful planning. In addition, the population of the Houston PMSA (a 6-county area) grew at a rate of 25.8% between 1990 and 2000, well above the national growth rate of 13% (U.S. Census Bureau, 2001; 2000; 1995). To accommodate, residential developments are built in an ever expanding circle around Houston's central business district. Most of these new developments completely clear an area of vegetation (tree canopy) prior to construction. After construction is completed, the new residents plot lawns and plant small trees where large ones once stood. Not only does this urbanization contribute to the overall man-made heating in the Houston area, it also creates a 'micro-urban heat island' effect (Aniello et al., 1995).

Micro-urban heat islands are smaller areas that display a relatively higher temperature than their immediate surrounding areas. They have a center point at which the temperature is highest and from which they radiate out (Aniello et al., 1995). The larger urban heat island can exhibit temperatures 4 to 6.5° C higher than their

surrounding rural areas (Streutker, 2002; Matson et al., 1978). In a similar fashion, smaller scale micro-urban heat islands have been documented to be as high as 5 to 11° C warmer than tree-shaded areas immediately surrounding them. For newer residential areas that have been cleared of tree canopy during construction, the same micro-urban heat island effect can be observed by evaluating a thermal image with a relatively high spatial resolution like Landsat ETM+ (60 meters).

Houston has a model that can be used to contrast a residential development style that clears land of vegetation prior to construction against one that endeavors to preserve tree canopy during construction: the Lake Houston neighborhood and The Woodlands respectively. Examining the thermal images of these two large residential areas allows for a clear contrast in temperature to be visualized. The tree canopy that could provide a cooling effect in the Lake Houston neighborhood has been removed and replaced with pavement and homes or residential lawns and low-level vegetation. The Woodlands has an extensive tree canopy providing an apparent cooling effect for the neighborhood. Using this model, this research has examined smaller representative residential areas with varying amounts and types of vegetation that are in close proximity to each other. High-resolution DOQQs, LIDAR data, and Landsat ETM+ thermal data have been used to study the impact of residential-structure (a mix of vegetation types, amounts, and combinations and made-made features) on surface temperature.

The negative correlation between NDVI and surface temperature reveals that higher levels of green vegetation mitigate the urban heating effect (Lo & Quattrochi, 2003; Lo et al., 1997; Aniello et al., 1995). Considering, however, that residential land-

use (function) is made up of many different land-cover (form) types, the NDVI value alone does not provide detailed information about the residential-structure of a neighborhood, especially at relatively lower spatial resolutions like that of Landsat ETM+ (30 meters). Therefore, an NDVI may not be the best surrogate variable to quantify the independent influences that varying vegetation types, amounts, and combinations have on surface temperature at a micro-scale.

This study has employed a micro-scale vegetation measurement technique and a mix of differing proximal residential sample areas to define residential-structure and quantify the contribution that tree canopy and low-level vegetation separately have on observed temperature variations. This information can be utilized to help instruct developers and city planners concerned with the negative impacts of urban and suburban heating. It could also provide a scientific basis for urban planning programs that can be implemented at a neighborhood level, related the planned planting of trees, local building design codes, and new land development styles and practices for Houston.

By first examining two representative residential areas, it became clear that the mix of vegetation can explain the difference in temperature observed for these two relatively small neighborhoods. The neighborhood that had an abundance of tree canopy was much cooler (3º C) than the neighborhood that exhibited mostly low-level vegetation (lawns, low-lying plants, and small trees). Considering the fact that these two neighborhoods are only 1,200 meters apart, climate variability and elevation was not a factor. The contrasting residential-structures represent a micro-scale version of the dynamics observed in The Woodlands and the Lake Houston neighborhood.

With the information that was gleaned from the two representative residential regions, a micro-scale measurement approach was created that defined Total Vegetation Cover and Tall Tree Canopy from a high-resolution false color near-infrared composite DOQQ (1m) and LIDAR feature height data, respectively. This is accomplished using a thresholding technique (Lillesand et al., 2004). To further define the residential-structure, a masking process was employed to define High NDVI Tree Canopy, Total Tree Canopy, and Low-Level Vegetation (DeMers, 2002). A GIS was used to create a fishnet grid that demarcates and identifies 442 stratified random residential sample area with a variety of residential-structure types. Each micro-scale vegetation measurement was extracted for each sample area (in terms of the percent of area covered by a certain vegetation type) by means of a binary grid, and a simple programming function written in C++. Finally, the extracted statistics were plotted against temperature, and simple linear regression and multiple regression analysis techniques were used to quantify residential-structure and the response from surface temperature at a neighborhood scale.

The simple linear regression analysis results show that the Total Tree Canopy as measured can explain approximately 79% of the observed variation in surface temperature (R^2 = 0.7879). In addition, the regression equation provides that a 1% change in the area covered by Total Tree Canopy in a residential neighborhood will yield a temperature change of approximately ±0.061 Kelvin. This correlation was much stronger than correlation between temperature and the Total Vegetation Cover measurement (R^2 = 0.2766), indicating that the vegetation cover alone is a poor explanatory variable for surface temperature. The Total Tree Canopy correlation was

only slightly better than the correlation between temperature and the 2000 Landsat ETM+ mean NDVI values (30 meter resolution) for each sample area (R^2 = 0.7675), explaining approximately 77% of the variation in temperature. From the NDVI correlation results, it is clear that a high NDVI value is desirable in regard to lowering temperatures; however, the residential-structure that is needed to obtain a desired cooling effect in an individual neighborhood cannot be ascertained from the NDVI value alone.

Considering that low-level vegetation is present in a residential neighborhood along with the tree canopy, simple linear regression cannot provide the independent contributions of tree canopy and that of low-level vegetation cover toward lowering temperature as they act together. This was accomplished using multiple regression analysis. Two micro-scale vegetation measurements represent the explanatory variables: percent of area of Total Tree Canopy and percent of area of Low-Level Vegetation. The response variable is effective at-satellite surface temperature. By utilizing multivariate regression analysis, the independent contributions that both variables have on surface temperature can be quantified, even though they are in the same area.

Results show that these two micro-scale vegetation measurements, in terms of percent of area, can explain about 81% of the variation in surface temperature (R^2 = 0.813, Pearson's r = -0.902). This is a slight improvement over the simple linear regression correlations; however, the multivariate equation provides a quantitative value for the level of influence that each of the micro-scale vegetation measures separately has on temperature. The demand for information concerning the effects of urban and

suburban development is growing as the urban heating effect grows. Understanding the contribution that both tree canopy and low-level vegetation (lawns, small trees, and low-lying plants) have together and separately on the mitigation of the heating effect in residential areas can provide neighborhood planners with needed information to design a sound residential-structure. It is evident that by selecting a certain residential development style, a developer or city planner can greatly influence the thermal properties of the new neighborhood (e.g., The Woodlands and the Lake Houston neighborhood). A developer must have specific information concerning residential-structure if goals to meeting a certain level of micro-urban heat mitigation or reduction are to be met.

With a quantified description of the influence that a certain residential-structure has on temperature, a proper combination can be planned that will allow for lawns and new small trees, but will also retain a certain amount of the older tree canopy during construction. The multiple regression equation (explanatory equation) provides that quantified description: increasing or decreasing the Total Tree Canopy by 1% will yield an expected change in temperature of approximately ±0.069 Kelvin, and by in increasing or decreasing the Low-Level Vegetation by 1%, a change of approximately ±0.023 Kelvin can be expected. Furthermore, the equation indicates that although low-level vegetation has some significant mitigating effect on temperature, it is almost three times less than that of tree canopy. While the desire for lush, green lawns free of pine needles is appealing, it should be understood that low-level vegetation is not as effective in cooling the neighborhood. In addition, the shade and cooling effect that tree canopy

provides can also create an appealing environment: three times more appealing in regards to micro-urban heat mitigation.

The 442 residential sample areas analyzed in this study represent a variety of residential-structure types, amounts, and combinations. The larger study area that contains these sample areas was chosen because of the variety it presented. A similar study that used feature height values for a more homogeneous area might find that the feature heights were less significant. For example, a completely forested area would provide little variation in feature heights and yield a less statistically significant result. The results would be as inconclusive for an area that was mostly grassland or low-level vegetation. In addition, this type of study would most likely yield results that were just the reverse if conducted in a purely urban environment with taller buildings.

However, the threshold values could be adjusted to different residential areas and for different seasons. The taller trees that did not have a high NDVI value were retained as a part of the tree canopy. This decision was based on the fact that the vast majority of the residential homes in the larger study area were less than 25 feet high and the fact that much of the observed tree canopy would have gone unmeasured. As noted, however, some sample areas had taller homes that registered as tree canopy, given the threshold value. Although this was rare, it does reflect a certain level of error and an opportunity for adjustment. Various threshold levels could be tested for both the feature heights (Tall Tree Canopy) and the NDVI (Total Vegetation Cover).

Considering that the NDVI threshold came from a 1995 DOQQ, the feature height values came from 2001 LIDAR data, and the thermal information came from

2000 Landsat ETM+ imagery, many of the potential residential sample areas had to be rejected. These were areas that showed change in residential-structure between 1995 and 2000 and represented many of the newer residential developments. In general, these areas exhibited relatively higher temperatures, and the need to evaluate these areas remains important. A large portion of the accuracy of the estimates is dependent upon the amount of change in a region between 1995 (NDVI acquisition) and 2001 (LIDAR acquisition). Therefore, a careful assessment of each sample area was conducted. The use of temporally correlated NDVI and LIDAR data and/or a highly accurate LULC map could provide a more automated means by which to identify purely residential sample areas and eliminate a certain degree of inaccuracy. That being said, a study that utilized the differences from one year to the next observed by the DOQQs could be used to evaluate the change in temperature at high resolutions for new developments regarding the removal of tree canopy and the increase in temperature or the micro-urban heat island effect, which may be illuminating.

The spatial resolution for the thermal data used in this study is 60 meters from the Landsat ETM+ imagery, which is relatively high for thermal data in general and it is widely available. Moreover, the delineation and quantification of tree canopy utilizing remotely sensed data at higher spatial resolutions (DOQQ and LIDAR) have enhanced the thermal data obtained from the Landsat imagery and have provided the means to study urban heat islands at a neighborhood level. However, the use of high-resolution thermal data, like that provided by the ATLAS (5 to 10 meters) could greatly enhance

this type of study, albeit, high-resolution ATLAS data is rarely available and not available for the Houston Metropolitan Area.

Future research could define residential-structure more in terms of quantifying the man-made features. The use of information from city planning offices or real-estate databases could yield an exacting variable for the size of the human footprint in residential areas. In addition to the micro-scale vegetation measurements, coupling the man-made element into the equation in a more precise manner would produce results that provide an even more informative guide to decision-makers or developers with respect towards policy or planning implementation for residential land development.

Remote sensing technologies have allowed researchers the ability to study large areas of terrain at greater levels of detail (Jensen, 2000). This study has focused on the influence of residential-structure on micro-scale urban heating. Larger scale studies have effectively defined and measured urban heat islands for whole cities (Streutker, 2003; 2002; Lo & Quattrochi, 2003; Lo et al., 1997). However, many of the factors contributing to the larger city-wide urban heat island problem occur at a neighborhood level and have an accumulative effect. The residential area required to support larger cities is ever growing; and population and urban densities also continue to increase. Although not scientifically validated as yet, heat islands may be more the products of urban design than merely density of development (Estes et al., 2003). By examining residential areas and the impact that various types, amounts, and combinations of vegetation have on surface temperature, this research has designed and quantified micro-

scale vegetation measurements that prove to be statistically significant variables that explain the observed variation in temperature in residential neighborhoods.

The strong negative correlation that NDVI has with temperature has been clearly shown in this study as well as many others. In addition it is well understood that a low NDVI value in a neighborhood will have an overall beneficial effect in regard to lowering temperatures. However, the specific type of residential-structure needed to obtain an overall high NDVI value has been less well established. The explanatory variables derived from this study may move decision-makers and developers toward a better understanding of the impact of residential-structure as a positive or negative factor on the environment and quality of life for an ever growing percentage of the world's population (Lo & Quattrochi, 2003; Berry, 1990; Cardelino & Chameides, 1990).

Monitoring, measuring, and understanding spatial patterns and factors contributing to large scale urban heat island effects are essential for formulating guidelines, standards, and sound public policies aimed at mitigating and avoiding the adverse environmental impacts of urban heat islands. That being said, deforestation and urbanization resulting in micro-urban heat island problems occur at the neighborhood level and contribute to the overall urban heat island problem. Given the fact that many residential developers continue to clear the land completely before they begin construction, a clear understanding of the impact, the potential benefits, and a measurable cause and effect guide might provide the tools and opportunity for those forward thinking entrepreneurs to promote and market their new residential development as a "COOL" neighborhood. This would be a neighborhood that could offer its residents

homes that require less energy to cool, relative to homes in other residential developments. Due to the lower temperatures, air conditioner use would be reduced and the energy bills that a resident must pay every month would be decreased. In addition, these "COOL" neighborhoods would offer a greater amount of tree canopy, which is most often considered aesthetically pleasing and generally increases the property values of homes by making them more desirable at market.

In summary, this research has: 1) improved our understanding of the factors and mechanisms contributing to the formation and development of urban heat islands; 2) enhanced our knowledge of the micro-urban heat island effect; 3) demonstrated the capabilities of assessing urban and suburban heating with high-resolution remotely sensed imagery and LIDAR feature height data; 4) improved our understanding of the impact of residential-structure in regards to the general urban heat island effect; and 5) explored the possible uses of this information for guiding future developers and policy-makers. "By utilizing sound urban planning, a city can avert or alleviate the effect of urban heat islands" (Lo et al., 1997). Ultimately, expanded research regarding optimal ratios between micro-urban heat islands (impervious built-up surfaces) and vegetative cover (tree canopy) could reveal an exacting residential-structure that nearly eliminates the contribution that residential development makes toward the larger urban heat island problems that afflict large cities.

REFERENCES

Akbari, H. (2002). Shade trees reduce building energy use and CO_2 emissions from power plants. *Environmental Pollution*, *116*, S119-S126.

Aniello, C., Morgan, K., Busbey, A., and Newland, L. (1995). Mapping micro-urban heat islands using Landsat TM and a GIS. *Computers & Geosciences*, *21*, 965-969.

ATLANTA. (2004). Remote Sensing. Urban Climatology and Air Quality. Project ATLANTA. Available at: http://wwwghcc.msfc.nasa.gov/atlanta/urban_atlanta_research.html.

Berry, B.J.L. (1990). Urbanization. In *The Earth as Transformed by Human Action: Global and Regional Changes in the Biosphere over the Past 300 Years*. B.L.I. Turner, W.C. Clark, R.W. Kates, J.F. Richards, J.T. Mathews, and W.B. Meyer (Eds.), New York: Cambridge University Press, 119-130.

BMS. British Meteorological Society. (2004). The 1850 and 1851 Membership Lists of the British Meteorological Society. The Royal Meteorological Society Available at: http://www.royal-met-soc.org.uk/pdf/metsocearlymembers.pdf.

Brandtberg, T., Warner, T.A., Landenberger, R.E. and McGraw, J.B. (2003). Detection and analysis of individual leaf-off tree crowns in small footprint, high sampling density lidar data from the eastern deciduous forest in North America. *Remote Sensing of Environment, 85*, 290-303.

Burt, J.E. and Barber, G.M. (1996). *Elementary Statistics for Geographers*, Second Edition. New York: The Guilford Press.

CAA. Clean Air Act. (2004). Air Quality Control Regions, Section 107, (d)(1)(A)(i). Available at: http://www.epa.gov/oar/caa/caa.txt.

Campbell, J.B. (2002). *Introduction to Remote Sensing,* Third Edition. New York: The Guilford Press.

Cardelino, C.A., and Chameides, W.L. (1990). Natural hydrocarbons, urbanization, and urban ozone. *Journal of Geophysical Research*, *95*, 13971-13979.

Clark, M., Clark, D.B., and Roberts, D.A. (2004). Small-footprint LIDAR estimation of sub-canopy elevation and tree height in a tropical rain forest landscape. *Remote Sensing of Environment, 91*, 68-89.

DeMers, M.N. (2002). *GIS Modeling in Raster.* New York, NY: John Wiley & Sons.

EPA. Environmental Protection Agency, U.S. (2002). Health and Environmental Effects of Ground-Level Ozone. July 11, 2002. Available at: http://www.epa.gov/ttn/oarpg/naaqsfin/o3health.html.

EPA. Environmental Protection Agency, U.S. (2000). 1997-1999 8-Hour Ozone County and Site Design Values. September 6, 2000. Available at: http://www.epa.gov/ttn/naaqs/ozone/areas/state/aq/aq99site.htm.

Estes, M., Jr., Quattrochi, D.A., and Stasiak E. (2003). The urban heat island phenomenon how its effects can influence environmental decision making in your community. *Public Management*. April, p. 8-12.

Flood, M., and Gutelius, B. (1997). Commercial implications of topographic terrain mapping using scanning airborne laser radar. *Photogrammetry Engineering and Remote Sensing, 63*, 327-329, 363-366.

Francois, C., and Ottle, C. (1996). Atmospheric corrections in the thermal infrared: Global and water vapor dependent split-window algorithms- applications to ASTER and AVHRR data. *IEEE Transactions on Geoscience and Remote Sensing, 34*, 457-470.

Gallo, K.P., and Tarpley, J.D. (1996). The comparison of vegetation index and surface temperature composites for urban heat island analysis. *International Journal of Remote Sensing, 17*, 3071-3076.

Gallo, K.P., McNab, A.L., Karl, T.R., Brown, J.F., Hood, J.J., and Tarpley, J.D. (1993). The use of a vegetation index for assessment of the urban heat island effect. *International Journal of Remote Sensing, 14*, 2223-2230.

GHCC. Global Hydrology and Climate Center. (1997). Airborne Thermal Remote Sensing Data Collected Over Atlanta. The GHCC Forecast, 3(8), May 16. Available at: http://wwwghcc.msfc.nasa.gov/Newsletter/0516.html.

Goudie, A. (2000). *The Human Impact on the Natural Environment*, 5th Edition. Cambridge: MIT Press.

Gregory, K.J. (2000). *The Changing Nature of Physical Geography*. London: Edward Arnold.

HARC. Houston Area Research Council. (2004). Cool Houston Project. Available at: http://www.harc.edu/harc/projects/coolhouston/.

Hellwich, O., and Ebner, H. (2000). Geocoding SAR interferograms by least squares adjustment. *ISPRS Journal of Photogrammetry and Remote Sensing, 55*, 67-72.

Henry, J.A., Dicks, S.E., Wetterqvist, O.F., and Roguski, S.J. (1989). Comparison of satellite, ground-based, and modeling techniques for analyzing the urban heat island. *Photogrammetry Engineering and Remote Sensing*, *55*, 69-76.

Howard, L. (1833). *The Climate of London*, Volumes I-III. London: Harvey and Dorton.

Jensen, J.R. (2005). *Introductory Digital Image Processing: A Remote Sensing Perspective*. Upper Saddle River, NJ: Prentice-Hall.

Jensen, J.R. (2000). *Remote Sensing of the Environment: An Earth Resource Perspective*. Upper Saddle River, NJ: Prentice-Hall.

Kawashima, S., Ishida, T., Minomura, M., and Miwa, T. (2000). Relations between surface temperature and air temperature on a local scale during winter nights. *Journal of Applied Meteorology*, *39*, 1570-1579.

Krabill, W.B., Collins, J.G., Link, L.E., Swift, R.N., and Butler, M.L. (1984). Airborne laser topographic mapping results. *Photogrammetry Engineering and Remote Sensing, 50*, 685-694.

Kustas, W.P., Norman, J.M., Anderson, M.C., and French, A.N. (2003). Estimating subpixel surface temperatures and energy fluxes from the vegetation index – radiometric temperature relationship. *Remote Sensing of Environment*, *85*, 429-440.

LBNL. Lawrence Berkeley National Laboratory. (2004). Heat Island Group. Available at: http://eetd.lbl.gov/HeatIsland/.

Li, F., Jackson, T.J., Kustas, W.P., Schmugge, T.J., French, A.N., Cosh, M.H., Bindlish, R. (2004). Deriving land surface temperature from Landsat 5 and 7 during SMEX02/SMACEX. *Remote Sensing of Environment*, *92*, 521-534.

Lillesand, T.M., Kiefer, R.W., and Chipman, J.W. (2004). *Remote Sensing and Image Interpretation,* Fifth Edition. New York, NY: John Wiley & Sons.

Lo, C.P., and Quattrochi, D.A. (2003). Land-use and land-cover change, urban heat island phenomenon, and health implications: A remote sensing approach. *Photogrammetric Engineering & Remote Sensing*, *69*, 1053-1063.

Lo, C.P., and Faber, B.J. (1997). Integration of Landsat Thematic Mapper and census data for quality of life assessment. *Remote Sensing of Environment*, *62*, 143-157.

Lo, C.P., Quattrochi, Dale A., and Luvall, J.C. (1997). Application of high-resolution thermal infrared remote sensing and GIS to assess the urban heat island effect. *International Journal of Remote Sensing*, *18*, 287-304.

Maas, H. (2002). Methods for measuring height and planimetry discrepancies in airborne laserscanner data. *Photogrammetry Engineering and Remote Sensing, 68*, 933-940.

Mann, K.J. (1993). Computer simulation of an urban heat island using finite elements. *Mathematics and Computers in Simulation*, *35*, 203-209.

Matson, M., McClain, P., McGinnis Jr., D., and Pritchard, J. (1978). Satellite detection of urban heat islands. *Monthly Weather Review*, *106*, 1725-1734.

Montávez, J.P., Rodríguez, A., and Jiménez, J.I. (2000). A study of the urban heat island of Granada. *International Journal of Climatology*, *20*, 899-911.

NASA. National Aeronautics and Space Administration. (2004). 11.3.1 Conversion to Radiance and 11.3.3 Band 6 Conversion to Temperature, Chapter 11 – Data Products. *Landsat 7: Science Data Users Handbook*. Available at: http://ltpwww.gsfc.nasa.gov/IAS/handbook/handbook_htmls/chapter11/chapter11.html.

Nelson, R., Krabill, W., and Tonelli, J. (1988). Estimating forest biomass and volume using airborne laser data. *Photogrammetry Engineering and Remote Sensing, 24*, 247-267.

Nichol, J.E. (1996). High-resolution surface temperature pattern related to urban morphology in a tropical city: A satellite-based study. *Journal of Applied Meteorology*, *35*, 135-146.

Nilsson, M. (1996). Estimation of tree heights and stand volume using an airborne LIDAR system. *Photogrammetry Engineering and Remote Sensing, 56*, 1-7.

Oke, T.R. (1987). *Boundary Layer Climates*. London: Routledge, 262-302.

Owen, T. W. Carlson, T.N., and Gillies, R.R. (1998). An assessment of satellite remotely sensed land cover parameters in quantitatively describing the climatic effect of urbanization. *International Journal of Remote Sensing*, *19*, 1663-1681.

Persson, A., Holmgren, J., and Söderman, U. (2002). Detecting and measuring individual trees using an airborne laser scanner. *Photogrammetry Engineering and Remote Sensing, 68*, 925-932.

Prata, A.J. (1993). Land surface temperatures derived from the Advanced Very High Resolution Radiometer and the Along-track scanning Radiometer 1, theory. *Journal of Geophysical Research*, *98*, 16689-16702.

Price, J.C. (1984). Land surface temperature measurements from the split window channels of the NOAA 7 AVHRR. *Journal of Geophysical Research*, *89*, 7231-7237.

Quattrochi, D.A. and Luvall, J.C. (2004). *Thermal Remote Sensing in Land Surface Processes*. D.A. Quattrochi and J.C. Luvall (Eds.), Boca Raton: CRC Press.

Quattrochi, D.A., Luvall, J.C., Rickman, D.L., Estes, Jr., M.G., Laymon, C.A., and Howell, B.F. (2000). A decision support information system for urban landscape management using thermal infrared data. *Photogrammetric Engineering & Remote Sensing*, *66*, 1195-1207.

Roth, M., Oke, T.R., and Emery, W.J. (1989). Satellite derived urban heat islands from three coastal cities and the utilization of such data in urban climatology. *International Journal of Remote Sensing*, *10*, 1699-1720.

Saaroni, H., Ben-Dor, E., Bitan, A., and Potchter, O. (2000). Spatial distribution and microscale characteristics of the urban heat island in Tel-Aviv, Israel. *Landscape and Urban Planning*. *48*, 1-18.

Sailor, D.J., Lu, L., and Fan, H. (2003). Estimating urban anthropogenic heating profiles and their implications for heat island development. In proceedings of the Fifth International Conference on Urban Climate (ICUC-5), Lodz, Poland, September 1-5.

Sakakibara, Y. (1996). A numerical study of the effect of urban geometry upon the surface energy budget. *Atmospheric Environment*, *30*, 487-496.

Schmugge, T., French, A., Ritchie, J.C., Rango, A., and Pelgrum, H. (2002). Temperature and emissivity separation from multispectral thermal infrared observations. *Remote Sensing of Environment*, *79*, 189-198.

Stone, B., Jr., and Rodgers, M.O. (2001). Urban form and thermal efficiency: How the design of cities influences the urban heat island effect. *Journal of the American Planning Association*, *67*, 186-198.

Streutker, D.R. (2003). Satellite-measured growth of the urban heat island of Houston, Texas. *Remote Sensing of Environment*, *85*, 282-289.

Streutker, D.R. (2002). A remote sensing study of the urban heat island of Houston, Texas. *International Journal of Remote Sensing*, *23*, 2595-2608.

Tannenwald, R. (1997). State regulatory policy and economic development. *New England Economic Review*. Federal Reserve Bank of Boston, March/April, 1997, 83-99.

TNRCC. Texas Natural Resource Conservation Commission. (2004a). The National Ambient Air Quality Standards. Available at: http://www.tnrcc.state.tx.us/air/monops/naaqs.html.

TNRCC. Texas Natural Resource Conservation Commission. (2004b). TCEQ Nonattainment and Near Nonattainment Areas. Available at: http://www.tnrcc.state.tx.us/gis/metadata/nonatain_met.html.

U.S. Census Bureau. (2001). Population Change and Distribution: Census 2000 Brief. Issued April 2001. Available at: http://www.census.gov/prod/2001pubs/c2kbr01-2.pdf.

U.S. Census Bureau. (2000). National 2000 Census. Available at: http://www.census.gov/main/www/cen2000.html.

U.S. Census Bureau. (1999). Metropolitan Areas and Components. Available at: http://www.census.gov/population/estimates/metro-city/99mfips.txt.

U.S. Census Bureau. (1995). Texas Population of Counties by Decennial Census: 1900 to 1990. Available at: http://www.census.gov/population/cencounts/tx190090.txt.

Vidal, A. (1991). Atmospheric and emissivity correction of land surface temperature measured from satellite using ground measurements or satellite data. *International Journal of Remote Sensing*, *12*, 2449-2460.

Voogt, J.A., and Oke, T.R. (1997). Complete urban surface temperatures. *Journal of Applied Meteorology*, *36*, 1117-1132.

Walsh, S.J., Evans, T.P., and Turner, B.L.I. (2004). Population-environment interactions with an emphasis on land-use/land-cover dynamics and the role of technology. In *Geography and Technology*. S.D. Brunn, S.L. Cutter, and J.W. Harrington Jr. (Eds.), Dordrecht: Kluwer Academic Publishers, 491-519.

Weng, Q., Lu, D., and Schubring, J. (2004). Estimation of land surface temperature – vegetation abundance relationship for urban heat island studies. *Remote Sensing of Environment*, *89*, 467-483.

Yamshita, S., and Sekine, K. (1990). Some studies on the Earth's surface conditions relating to the urban heat island. *Energy and Building*, *15-16*, 279-288.

VITA

Name: Matthew A. Clemonds

Address: 1600 Rebecca Lane, Arlington, Texas 76014

Email Address: mclemonds@msn.com

Education: M.S., Geography, Texas A&M University, College Station, 2005
                    4.0 GPA

                B.S., Geography, Texas A&M University, College Station, 2002
                    Summa cum Laude, 4.0 GPA.

                A.S., North Harris College, Houston, Texas, 2000
                    Summa cum Laude, 4.0 GPA.

Experience: 2003-present, Graduate Teaching Assistant
                    Texas A&M University

                2003-present, Research Assistant
                    Texas A&M University

                2003-present, Project Manager and Assistant
                    The Texas A&M University System

                2002, Research Assistant
                    Texas A&M University

                1990-1998, Master SCUBA Diving Instructor
                    Guam, USA

                1987-1991, Hospital Corpsman
                    United States Navy